

2018



**25th Congress of
International Federation for
Heat Treatment and Surface Engineering**

11-14 September 2018 | Xi'an China

PROCEEDINGS



Organized by Chinese Heat Treatment Society (CHTS)

25th IFHTSE CONGRESS PROCEEDINGS

11-14 September 2018

Xi'an China



Chinese Heat Treatment Society

Tel: +86 (0) 10 6292 0613 • Email: chts@chts.org.cn • Web: www.chts.org.cn

Add: 18 Xueqing Rd., Beijing, China

Very high cycle fatigue property of micro-shot peened EA4T axle steel.....	529
Effect of shot peening treatment on fatigue property of EA4T axle steel.....	529
Characterization and simulation of evolution of process-induced residual stress in Ni-based superalloy components.....	530
Experimental research on effect of cryogenic treatment on residual stress of 2024 aluminum alloy.....	530
Study on strengthening effect of extra magnetic field on the detection of cladding coatings residual stress based on magnetic memory testing.....	531
Residual stress evolution and distortion responds of 2024 Al alloy plate.....	531

Failure Analysis

Research on crack propagation in weld seam of spiral coil waterwall based on stress superimposed effect.....	532
Experience with Grade 91 DMW failures—features and current understanding.....	534
Failure analysis of gear on rail transit.....	535
Co-occurrence analysis of thermal power plant failure cases.....	536
Failure analysis of super 13Cr tubing in high temperature and ultra-deep sour gas well.....	537
Premature fracture failure analysis of boric acid recycle pump shaft in 1000 MW nuclear power plant.....	538
Mechanical shock tests and a failure analysis for pins of a stacked memory device in aerospace applications.....	539
Investigation on tensile failure of heat-treated rigid polyurethane foam by experiment and numerical simulation.....	540
Fracture failure analysis of the outer ring from a grease-lubricated cylindrical roller bearing in an air blower motor.....	542
Abnormal failure analysis of NiSiCr3552 cast exhaust manifold.....	544
Fracture failure analysis on the bottom side beam of Q355GNH container.....	545
New interpretation of materials failure analysis and its application.....	546
Corrosion failure analysis of 20/316L bimetal-lined pipe under strong acid environment.....	547
Failure analysis of quenching cracking of 45 steel flange.....	548
Failure analysis of TP92 steel piping.....	549
Failure analysis and prevention of heat-resistant alloy tube in petrochemical industry.....	549
Failure analysis of components and fracture mechanisms of metallic materials.....	550
Pipeline deformation and monitoring technology.....	550
Failure analysis of the balance ball pin in the car steering system.....	551
Failure analysis of an automotive bushing.....	551
Study the cases of the cracking failure of automobile steering knuckle.....	552
Failure analysis on leaked titanium tubes for seawater heat exchanger in recirculating cooling water system of coastal nuclear power plant.....	552

Design and test analysis of bionic subsoiler tip.....	553
Investigation on typical failure mode of high-pressure hydrogen storage tanks for vehicles.....	553
Failure analysis of regenerative gas electric heater outer wall cracking.....	554
The influence of copper on the stress corrosion cracking of 304 stainless steel.....	554
Influence of working temperature on the service behavior of tubing in water injection wells.....	555
Analysis and improvement of the cracking cause of the 50CrVA steel stabilizer rod of an automobile.....	555
Fatigue failure of a horizontal tail's hollow shaft of an aircraft—the impacts of surface integrity and stress concentration.....	556
Design and test analysis of bionic subsoiler tip.....	556
Failure analysis of a brass valve.....	557
Three fatigue failure analysis of gas cylinder for long tube trailer.....	557
Failure analysis on fractured carbon dioxide fracturing tube.....	558
Metallographic automatic rating technology and its application through machine learning.....	558
Pipeline failure analysis of phenol acetone.....	559
Failure analysis of drill pipe's rotary shouldered thread connection.....	559
The countermeasures of failure risk on strength performance of closing part for steel gate valve.....	560
Effects of TiN coating on the very high cycle fatigue properties of Ti-6Al-4V titanium alloy.....	560
Failure analysis on the cracking of girth weld joint of steam pipeline.....	561
Failure analysis on energy conservation equipment in waste heat boiler system.....	561
Failure analysis of 45 steel hydraulic cylinder ear.....	562
Mechanism of fault slippage and influence on casing deformation for horizontal shale gas wells.....	563
Evaluation of irradiation degradation of nuclear cable materials by the infrared microscope approach.....	564
Experimental study on mechanical and fatigue behavior of dissimilar friction stir welded joint.....	566
Failure analysis on abnormal combustion of transformers in offshore wind turbines.....	568
Magnetic plug fracture in gearbox of high speed train.....	569
Failure analysis of wear and tear on GCr15SiMn rolling bearing steel.....	570
Finite element simulation on the vibration failure of rigid polyurethane foam at high temperature.....	571
Numerical study of mechanical properties of straight pipe and elbow during in-service welding.....	572
Service experiences with cracking in T23 weldments.....	573
Thermally grown oxide (TGO) formation and growth in doublelayered composite thermal barrier coating and failure mechanism analysis.....	574
Failure analysis of excessive corrosion in wastewater treatment reactor.....	575
Failure analysis of angular contact ball bearing in a boosting pump of nuclear power plant.....	575

Failure analysis of leakage of valve tube in drain pipeline in nuclear power plant.....	576
Failure analysis of leaking small-diameter buried 20 steel pipe.....	576
Helical spring fracture failure analysis of suspension for vehicle.....	576
Peridynamic simulation of crack formation and propagation in pitting corrosion of carbon steel pipes.....	577
Failure case analysis—failure analysis of casing head slip hanger.....	577
Failure analysis of welded chain slings used for lifting purpose in oil and gas industry.....	578
Investigation on impact absorbed energy index of drill pipe.....	578
Failure analysis of sulfide stress corrosion cracking on P105 tubing coupling.....	579
Experimental study on temperature effect of high performance casing material in deep well and ultra-deep well.....	579
Fracture control of the 2nd west east gas pipeline.....	580
Fracture failure analysis on ultra supercritical turbine bolts.....	580
Research on the performance of hollow bolt yield ratio of 45 steel.....	581
Failure analysis of a P110 grade non-API anti-sulfide corrosion tubing coupling used in ultra deep oil well.....	581
A phase transformation to predict the high contact stress in bearing steel due to rolling contact fatigue.....	582
Cracking failure analysis on L245NS steel grade elbow.....	582
Fracture failure analysis of C110 casing in sour oil and gas field.....	583
EIS studies of the resistance-reducing internal coating of in-service natural gas pipeline.....	583

Microstructure and Properties

Effect of Si and Cr on surface microstructure formed by lithium doped salt-bath nitrocarburizing in Fe-0.4wt%C.....	584
Preparation of Mo ₅ SiB ₂ powder by mechanical alloying and annealing.....	585
The effect of twins and substructures evolution on dynamic recrystallization behaviors in Ni-30Fe austenitic alloy.....	586
The high-temperature tensile behaviors of vanadium-containing 25Cr-20Ni austenitic stainless steels.....	588
Effect of {332} <113> twinning on Charpy impact behavior in metastable β -type Ti-15Mo alloy.....	590
Fabrication, structure, and thermal stability of electroless Ni-Fe-P coating.....	591
Surface characterization of a selectively dissolved Ni-Ni ₃ Si eutectic alloy.....	592
Preparation of molybdenum copper composite powder by wet chemical method and its sintering properties.....	593
The effect of post-weld heat treatment on the carbide evolution of Hastelloy N alloy in heat affected zone.....	594
Effect of annealing temperature on texture and magnetic properties of 6.5%Si ultra-thin strip.....	594

Research on crack propagation in weld seam of spiral coil waterwall based on stress superimposed effect

Zhenrong Yan¹, Jun Si²

(1. Shanghai Boiler Works Co., Ltd.;

2. Shanghai Institute of Special Equipment Inspection and Technical Research)

yanzr2010@163.com

Abstract: The spiral coil waterwall is the core functional components of Ultra Supercritical Boiler. Operation practice and research show that the weld cracks on the waterwall are very common. However, the strength and metallographic structure nearby or in the weld cracks on waterwall are mostly to meet the requirements of the relevant standards.

In view of stress superimposed effect, this paper research the effect of various stresses on the weld crack propagation of waterwall. Firstly, it was used to the residual stress testing method, carried out the stress test on T23 spiral coil waterwall welded joint of 1000 MW ultra supercritical tower type boiler during the manufacture and installation, the results show that the welding residual stress reached about T23 tubes yield strength 70%, which is greater than allowable stress of T23 tube under working temperature (showed in Table 1 and Table 2). Secondly, stress numerical simulation method is used to carry out numerical simulation of welding residual stress, installation defect stress and working medium stress of spiral coil waterwall during operation. It was simulated that the installation and welding process of T23 waterwall tube in 1000 MW ultra supercritical tower boiler during the installation, and the residual stress field of the welding was obtained (showed in Fig.1). On the basis of these, put the load of the working medium on the spiral coil waterwall, the superimposed stress distribution of the welding residual stress and the stress of the working medium were obtained (showed in Fig.2). Considering the bending moment formed by stagger joint which is the commonest installation defects, the stress field distribution of butt welds in T23 waterwall tubes was obtained by applying bending moment on the basis of the stress field of the welding residual stress and the working medium stress (showed in Fig.3).

The results shows that the welding residual stress is greater than greater than allowable stress of T23 tube under working temperature, therefore, the effect of T23 heat treatment after welding to reduce the crack of T23 waterwall crack is obvious; The working medium load plays a great role in the hoop stress of the waterwall tubes, and promotes the cracks in the butt welds ;The axial stress on the waterwall tubes produced by the installation defect stress is also obvious, the stagger joint, and other installation defects are the main reason of crack propagation of spiral coil waterwall.

Keywords: ultra supercritical boiler, spiral coil waterwall, T23 steel, welding residual stress, installation defect stress, working fluid stress

Table 1 The welding residual stress reached about T23 tubes during the manufacture

No.	Test Site	State of Postweld Heat Treatment state	Residual Stress /MPa
1	Butt weld between Multi pass forging and Tubes	Welded	305,310,321,298,295
2	Butt weld between Multi pass forging and Tubes	Heat-treated	32,39,50,65,61
3	Fillet weld between Multi pass forging and Sealing plate	Welded	182,175,188,220,265,245
4	Fillet weld between Multi pass forging and Sealing plate	Heat-treated	22,26,28,39,40
5	Fillet weld between Spiral waterwall tube and Filling plate	Welded	255,260,278,298,304
6	Fillet weld between Spiral waterwall tube and Filling plate	Heat-treated	32,37,45,56,65

Table 2 The welding residual stress reached about T23 tubes during the installation

No.	Code name of Power plant	Test Site	Transverse residual stress/MPa	Longitudinal residual stress/MPa
1	B	Angle weld between the rigid transition beam and the tubes on the 1 horn, 59 m elevation	84,175,98,202,198	300,325,385,373,390
2	B	Angle weld between the rigid transition beam and the tubes on the 1 horn, 49 m elevation	28,28,52,109,-129	118,214,234,352
3	H	Angle weld between the rigid transition beam and the tubes on the 1 horn, 59 m elevation	28,39,55,74,87	45,75,102,117,131
4	H	Angle weld between the rigid transition beam and the tubes on the 1 horn, 49 m elevation	104,148,184,-83,-121	157,181,245,207,-371

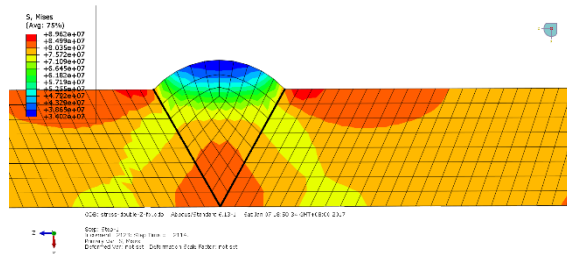


Fig.1 local residual stress field distribution in weld

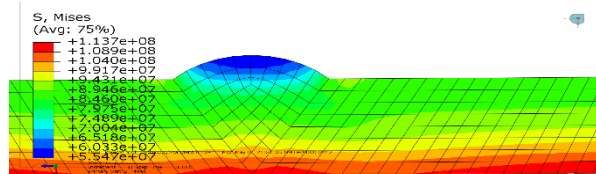


Fig.2 Stress distribution after superposition of the working medium load and welding residual stress

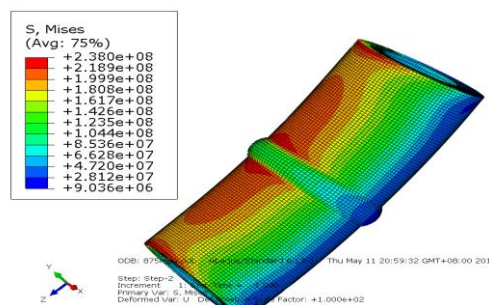


Fig.3 Stress distribution after superposition of the working medium load and welding residual stress as well as bending moment

Experience with Grade 91 DMW failures—features and current understanding

Gang Zhou

(ATC-Engineering Services)

jzhou@atc-tn.com

Abstract: Welds between engineering alloys of differing composition and thermo-physical properties, commonly referred to as dissimilar metal welds (DMWs), are an integral part of the equipment used in many advanced industrial processes, such as supercritical power plants and HRSGs. The great majority of DMWs are made to join components that operate at low or moderately elevated temperatures relative to the melting range of the alloys involved, and these welds routinely operate for long periods of time without incident. However, DMWs also are used in pressure part fabrication to join austenitic tubes or pipes to ferritic tubes or pipes or to join austenitic non-pressure part attachments to a ferritic tube or pipe. In these cases, the components of which the DMW is a part typically operate under conditions where creep damage coupled to the effects of frequent cycling is expected to influence the service life of the weld. Under these conditions, the performance of DMWs has been far less predictable. For example, the service history of DMWs made between low alloy ferritic tubing (e.g., Grade 22) and tubing fabricated from one of the 300-series austenitic steels (e.g., TP304H) and installed in superheaters (SH) or reheaters (RH) of large power boilers has been highly variable, depending critically on the choice of filler metal and, in certain cases, on the operating profile of the boiler. The reasons for the variability in performance now are understood to involve differences in the thermo-physical properties of the materials being joined as well as differences in local mechanical properties as these are altered by diffusion-driven compositional changes along the dissimilar metal interface. For the SH and RH DMWs, the response to the spate of early weld failures, where the weld was made using an austenitic stainless filler metal, was to switch to a nickel-base filler metal that minimized the incompatibility in the thermo-physical properties and reduced the local mismatch in mechanical properties by limiting the amount of carbon diffusion from the low alloy tubing into the more highly alloyed filler metal. The resulting two-to-threefold increase in the average service life of the DMWs underscored the basic soundness of the approach.

With this history in mind, when need arose to develop procedures for welding the creep strength enhanced steel Grade 91 to other alloys, and particularly to one of the austenitic stainless steels, the default choice of filler metal was, again, a nickel-base alloy. Since that decision was made, the frequency with which DMWs involving Grade 91 have failed after only relatively short periods of operation has drawn attention to the fact that the relative level of incompatibility between Grade 91 and other alloys clearly is even greater than was the case when low alloys such as Grade 22 constituted the ferritic component of the joint. Recent studies of failed DMW joints involving Grade 91 have confirmed that the failures are related not only to the fundamental welding metallurgy, but also to component manufacture, unit design, and the nature of the service. This paper reviews and summarizes what can be considered typical macroscopic and microscopic characteristics of the failures, including metallographic and fractographic features and compositional features, of the Grade 91 DMW failures and provides a hypothesis of the damage mechanism.

Keywords: Gr 91, dissimilar metal weld, failures

Failure analysis of gear on rail transit

Anxia Pan¹, Zhenguo Yang², ShiYuan Liu¹, Luoping Xu¹

(1. CRRC Qishuyan Institute Co., Ltd.; 2. Department of Material Science, Fudan University)
pax508@126.com

Abstract: In recent years, with the rapid development of rail transit in China, unprecedented achievements have been achieved both in mileage and construction scale, which has played a significant role in relieving urban traffic congestion and environmental pollution, generating immeasurable social and economic benefits. The gear transmission system is the key equipment for power transmission of the railway vehicle with regard to safety. Thus the failure analysis of gears is an important part in improving system reliability. This research describes four typical failure cases about gears in rail transit gearbox. Detailed studies including visual inspection, scanning electron microscope (SEM) and energy dispersive spectrum (EDS) analysis were performed on the damaged gears to determine the root causes for failure.

Case I: A locomotive gear shaft, the material is 20CrMnMo, had been heat treated with carburizing and quenching. However, longitudinal cracking occurred when the gear was in the final quenching. Conclusions of the failure analysis show that Al₂O₃ inclusions existed in a depth of about 5 mm beneath the surface of the gear shaft, which changed the stress distribution of the sub-surface of the gear shaft during the heat treatment, resulting in cracking of the gear shaft.

Case II: A driving gear was suffered fatigue cracking during operation about two months after the it had been loaded. Conclusions of the failure analysis show that the atmosphere was not properly controlled during the carburizing process of the gear, alloy oxides formed in the grain boundaries, thereby excessive troostite and grain boundary oxidation occurred on the surface, causing decreased surface hardness, significant decline in the fatigue strength and premature fatigue fracture influenced jointly by the service stress and the interference stress.

Case III: A driven gear of a high-speed train had been heat treated with induction hardening, an arcuate crack was found on the tooth surface after two years of service. Conclusions of the failure analysis show that the surface of gear has crescent-shaped “black spots” due to the improper grinding process, and that, the lower the hardness of the “black spot” is, the lower the surface stress state is, which is the main cause of fatigue peeling cracks on the tooth surface.

Case IV: The mating surfaces of the driving and driven gears of a locomotive are damaged, leading to a belt-shaped rough portion. Conclusions of failure analysis show that the damage morphology of the mating surfaces of the driving and driven gears conforms to the characteristics of hot scuffing. They are caused by the insufficient supply of lubricating oil, which leads to overheating of the gear meshing and rupturing of the oil film, causing adhesion and the resulting failure.

Based on the analyses of different causes of several gear failure cases on rail transit, the common factors leading to gear failure are discussed. It is concluded that the main factors causing premature failures of gears include substandard raw materials, improper heat treatment, flawed manufacturing process and irrational use. The relationships between each of the above factors and the gear failure are analyzed and discussed respectively, providing a theoretical basis for improving the gear life and reliability.

Keywords: rail transit, gear, failure, slag, grinding, cracking

Co-occurrence analysis of thermal power plant failure cases

Jiahui Lv, Weize Wang, Shaowu Liu

(East China University of Science and Technology)

wangwz@ecust.edu.cn

Abstract: Thermal power plant is the main power supply of our country, accounting for 70% of the total power generation. Demands on the thermal efficiency increase in power plants have led to an increase in pressure and temperature of steam, which causes component failures to grow. The safety and economy of thermal power plant have been influenced by the failure, so it is necessary to find out the cause of the failure and propose the corresponding measures to prevent the recurrence of similar failures.

This study focuses on surveying the failure cases in thermal power plant, which were extracted from journal papers on thermal power plant failure cases issued in China Academic Journal Network Publishing Database, and summarizes some failure rules on the basis of failed components, failed materials, as well as failure modes. First, a professional dictionary including keywords related to these three items was made to identify the keywords in each failure case. After extracting the keywords, co-occurrence analysis has been an effective method to discover interesting knowledge patterns from the association of keywords. Co-occurrence matrix needed to be built in the first place, and the edited programs were used to count the keywords frequency. It also visualized the results at every process of the research. Co-occurrence network set up by Ucinet and Netdraw, co-occurrence clustering analysis by SPSS, internal relations among high frequency keywords were studied. From the co-occurrence network, the larger the node in the network, and the higher the centrality is, which means the keywords is more important. And the thickness of the connection between nodes indicates the frequency of occurrence of the two groups of keywords. The higher the frequency, the more closely the keywords are. In the co-occurrence network, boiler tubes and rotating machinery are two of the biggest nodes. Boiler four tubular damage and leakage impacting on safe operation of the unit is the most common accident of the thermal power plant. And the rotating machinery is the second highest failure components, including the steam turbine, the generator, as well as the pump. According to the failures by material, carbon steel tubes lead as the most frequent materials causing failures. In the co-occurrence network, the thickness of the connection represents the correlation between the keywords. And the result shows that among boiler tubes, superheater tubes are the first highest failed components. In terms of failure modes, superheater tubes and reheater tubes are greatly related with high temperature creep, short-term overheating and dissimilar weld joints. As for water wall tubes, short-term overheating, hydrogen damage and thermal fatigue are the most common failure modes. Low- temperature corrosion and wear are greatly related with economizer failures. What's more, the elbow and welds are the typical failure location. The most related failure mode to rotating machinery is fatigue. As for the steam turbine, the dezincification corrosion of the condenser is remarkable other than the rotating parts. Since the failure of boiler pipe and rotating machinery can strongly influence the safety and economy of the thermal power plant, these weaken parts should be paid more attention during the operation, inspection and maintenance.

Keywords: thermal power plant, failure cases, co-occurrence, boiler tubes, high-temperature creep

Failure analysis of super 13Cr tubing in high temperature and ultra-deep sour gas well

Zhi Zhang¹, Yushan Zheng¹, Jing Li¹, Wanying Liu¹, Mingqiu Liu², Pengfei Sang¹

(1. Southwest Petroleum University; 2. Traim Oilfield Company of Petro China)

414897560@qq.com

Abstract: In the high temperature and ultra-deep sour gas well, super 13Cr is the most crucial component of wellbore configuration. This paper focus on super 13Cr tubing stress corrosion cracking (SSC) failure in the northwest area oilfield of China. The high temperature and ultra-deep sour gas well was produced about 2 years, and the tubing was failed approximately at 5000 m. In the annular pressure test, the pressure of annulus A was rapidly increased to 40 MPa, the pressure of annulus B and C were also boosted to 24 MPa and 20 MPa, respectively. In this case, the well was permanently abandoned because the failed tubing causes sustained casing pressure.

In this study, the failed tubing was investigated by the following procedures to assess corrosive attack:

1) Examination of outer surface by FMPI test. 2) Corrosion environment analysis by XRD test. 3) Mechanical properties test. 4) Morphological analysis of the tensile fracture surface. 5) EDS and XRD analysis of corrosion product. 6) OP and SEM analysis of tubing cracking.

First of all, the outer surfaces of tubing were examined by fluorescent magnetic particle inspection (FMPI) test, a large number of microcracks was taken using the camera. Furthermore, the sample pieces were cut from the failed tubing according to the requirements of different tests.

The chemical composition of format annulus protective solution was investigated by X-ray diffraction (XRD) test. The mechanical properties of the failed specimens were analyzed by tensile fracture test. The inclusion and metallographic structure were observed using optical microscopy, scanning electron microscopy (SEM) was also utilized to investigate the morphology of the tensile fracture surface, energy dispersive spectrometer (EDS) was used to analyze the relative content of chemical elements in the corroded surfaces, and X-ray diffraction (XRD) was used to analyze the composition of corrosion products.

Because the corrosion medium is CO₂ in the wellbore, the possible corrosion mechanism is as followed.

The anode reaction is: $\text{Fe} \rightarrow \text{Fe}^{2+} + 2\text{e}^-$; $\text{Fe} + \text{HCO}_3^- \rightarrow \text{FeCO}_3(\text{S}) + \text{H}^+$.

The cathode reactions include the reduction of H₂O and HCO₃³⁻: $2\text{H}_2\text{O} + 2\text{e}^- \rightarrow 2\text{OH}^- + \text{H}_2$; $2\text{HCO}_3^- + 2\text{e}^- \rightarrow \text{H}_2 + 2\text{CO}_3^{2-}$.

The hydrogen carbonate, HCO₃³⁻, has a greater influence for the cathodic reactions. When the pH of the solution is less than 4, the main cathode reaction is the reduction of H⁺, and the reaction rate is controlled by diffusion. When the pH of the solution is between 4 and 6, the main cathode reactions are the reduction of HCO₃³⁻ and carbonic acid, H₂CO₃, and the reaction rate is controlled by activity. When the cathode overpotential is high, the reduction of H₂O is the main cathode reaction.

Through investigation the fracture of super 13Cr tubing, the reason of the tubing failure is stress corrosion cracking which corrosion product film is breaking. Stress corrosion cracking will occur due to the cycle of corrosion product film rupture, metal matrix dissolution, and corrosion product film rebuilding. The concentrations of the element O and P are increased on the crack surface, which indicates these two elements play an important role in the crack growth.

Keywords: super 13Cr, stress corrosion crack, failure mechanisms

Premature fracture failure analysis of boric acid recycle pump shaft in 1000 MW nuclear power plant

Tongwei Ni¹, Qun Ding¹, Zhenguo Yang¹, Honglian Zheng², Xiao Lou²

(1. Department of Materials Science, Fudan University;

2. CNNP Nuclear Power Operations Management Co., Ltd.)

zgyang@fudan.edu.cn

Abstract: As an important equipment for maintaining the circulation of boric acid solution, boric acid recycle pumps (hereinafter referred to as boric acid pumps) plays an important role in keeping the safety of nuclear power plant. However, with the continuous progress of nuclear technology, the boric acid pumps is exposed to relatively complicated circumstances, such as corrosive media, high-speed rotation, atmospheric salt fog and so on. Under such conditions, the boric acid pumps may encounter unexpected failures, causing potential nuclear safety problem. Therefore, its operation safety and stability are facing severe challenges.

The case studied in this paper was about an unexpected failure of the boric acid pump, which happened in a 1000 MW nuclear power plant. The boric acid pump made by a Japanese company is a canned motor pump, and was officially put into service in 2014 with designed service life of 40 years. However, the pump could not work during the start-up process after serving for only one year. After disassembling inspection, the pump shaft was found to be broken at the front end of the shoulder. Since the failure of the boric acid recycle pump shaft has not been reported, the root reason for the premature fracture of the pump shaft should be definitively identified to ensure nuclear safety.

In order to ascertain the root reason of the failure, material identification, metallographic inspection, mechanical property test, fractographic observation, micro-zone analysis and mechanism analysis were carried out. Specifically speaking, the results of material identification, metallographic inspection and mechanical property test showed that the shaft are qualified 316L stainless steel. Fractographic observation and micro-zone analysis found that micro-cracks nucleated and coalesced around the inclusions. Mechanism analysis showed that the torsional shear stresses and bending stresses was not sufficient to cause the fracture of the pump. Given the fact that small transition arc radius, surface defect and inclusions aggregation were found at the fracture location, the root cause was proved to be the triple stress concentration.

Under the effect of the triple stress concentration, micro cracks nucleated and coalesced at the positive side near the front end of the shoulder, resulting in the initiation of cracks. Then cracks propagated clockwise along the circumferential direction under the joint effect of tensile stresses and torsional shear stresses. After that, when the residual cross section could not withstand external load with the propagation of the cracks, cracks got into transient fracture zone, leading to the premature fracture of the pump.

Based on the above analysis and conclusion, several useful countermeasures are came up with to solve relevant problems.

1) To achieve the aim of reducing the triple stress concentration, transition arc radius between the shaft and shoulder should be enlarged. At the same time, the surface after machining is supposed to be polished. In addition, the material quality of the shaft needs to be improved.

2) For the propose of reducing bending stresses, spline should be replaced by flat key.

3) To improve stiffness of the pump, the outer diameter of the shaft could be increased properly.

Keywords: failure analysis, boric recycle acid pump, triple stress concentration, special defects

Mechanical shock tests and a failure analysis for pins of a stacked memory device in aerospace applications

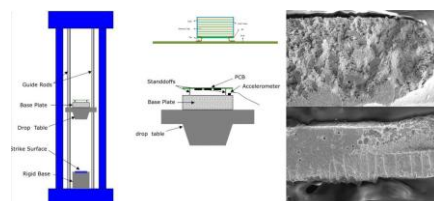
Xin Tao¹, Liyou Zhao², Jun Wang¹

(1. Department of Materials Science, Fudan University; 2. Shanghai Academy of Aerospace Technology)
jun_wang@fudan.edu.cn

Abstract: The memory devices are necessary in electronic systems of aircraft in aerospace applications. With the requirements of higher performance, the capacity of memory is expanded by stacked multiple devices into one package. Owing to increase of device weight, the pins and solder joints of the stacked memory device will sustain larger stresses under a mechanical shock that takes place frequently in the transportation, launching or flying of aircrafts. The soldering pins could be damaged under a large stress, which leads to malfunction of the system due to the open circuit of pins. The issues will endanger the security of flight. In this study, we tested the pins and solder joints of a stacked memory device on board-level by different conditions of mechanical shock and performed the failure analysis for the failed joints of devices.

In order to evaluate the integration of pins and solder joints of a stacked memory device under a mechanical shock, the device was assembled on a printed circuit board (PCB) by a surface mount technology. The board-level test was followed the standards of GJB548B2005 and JESD22-B111. A daisy chain was designed and implemented on the PCB, which linked all pins. The electrical connections of pins were evaluated by monitoring the transient and static resistance changes of the daisy chain both. The loading of a mechanical shock was applied by the tester dropped from a height. Two different conditions of mechanical shock, i.e. peak accelerations of 1500 g and 600 g, were used in this investigation. The applied acceleration curves are adjusted to meet the demand of the standards. The sketches of a mechanical shock test are demonstrated in Fig.1(a) and the assembled device is illustrated in Fig.1(b). The test results show that the device completely failed after four mechanical shocks at a peak acceleration of 1500 g. When the peak acceleration is decreased to 600 g, the device failed after 478 mechanical shocks. The mechanical shock gave rise to a large stress in the solder, which even made the device fall off from the PCB due to fractures of pins or solder joints. The failure analysis was carried out for the failed devices. Most failures occurred at the solder joints, especially the outmost ones. The failure modes of pins and solder joints caused by a mechanical shock were summarized. The morphologies of fracture for the two conditions with peak accelerations of 1500 g and 600 g are distinct from each other. The images of SEM in Fig.1 show the fracture surface of the damage solder joints. The surface is rough with many dimples for the case of 1500 g in Fig.1(c), which means a brittle fracture occurs. For the case of 600 g, the fracture surface is more smooth and contains some steps in Fig.1(d), which indicates fracture propagates gradually. The elements distributed information by a composition analysis on the fracture surface helps to identify the fracture locations. For example, the crack occurred at the middle of solder when the major elements are Pb and Sn. Some areas contain elements of AU and Ni, which are plated on the surface of the pad. It means the crack occurred near the intermetallic compound (IMC) layer. Following the rules, the typical fracture propagation path is delineated.

Keywords: failure analysis, mechanical shock, fracture, solder joint, stacked memory device



Investigation on tensile failure of heat-treated rigid polyurethane foam by experiment and numerical simulation

Yannan He, Zhiqiang Yu

(Fudan University)

yuzhiqiang@fudan.edu.cn

Abstract: The heat treatments of rigid polyurethane foams (RPUFs) were performed at different temperatures, and tensile properties of treated RPUFs were both studied by the experiments as shown in Fig.1 as well as numerical simulation.

The tensile stress-strain curves of RPUFs before and after treatment obtained from experiment were shown in Fig.2. It can be seen that after treatment with high temperature, the RPUFs were aged and the tensile strength and modulus of them decreased with the increase of treatment temperature. In comparison, the untreated RPUF had the highest tensile properties, and the tensile strength and modulus of it can reach 2.205 MPa and 14.00 MPa, respectively. The main reason which led to the aging of RPUFs is the expansion of cell size which caused by the degradation of polyurethane matrix according to the results of thermal gravimetric analysis (TGA) of untreated RPUFs which shown in Fig.3. According to the TG and DTG curves in Fig.3, the preliminary degradation of RPUFs such as random broken of macromolecules occurred at the range from 150 °C to 200 °C. It made the wall of cellular structure in the RPUFs decompose and cannot bear more external load, which resulted in the decrease of tensile properties of RPUFs.

Finite element analysis (FEA) of tensile properties of RPUFs were carried out by Cellular Structure Model (CSM) constructed according to the Kerner-Rusch relation shown in Eq.1 and Entire Bulk Model (EBM) constructed according to the Polynomial Relation of strain potential energy shown in Eq.2, respectively.

$$\frac{E_f}{E_0} = \frac{12\varphi}{23-11\varphi} \quad (1)$$

Where the E_f and E_0 are the Young's modulus of foams and matrix materials, respectively, and φ is the volume ratio of matrix materials.

$$U = \sum_{i+j=1}^N C_{ij} (\bar{I}_1 - 3)^i (\bar{I}_2 - 3)^j + \sum_{i=1}^N \frac{1}{D_i} (J_{el} - 1)^{2i} \quad (2)$$

Where the U is strain potential energy, and J_{el} is the elastic volume ratio. \bar{I}_1 and \bar{I}_2 are the deformation measurement of materials. N , C_{ij} and D_i are the materials parameters related to temperature.

In the CSM, the porosity of RPUFs can be calculated by the Young's modulus of RPUFs and polyurethane matrix according to Eq.1. And the cell with a certain size and quantity was constructed in CSM according to the porosity. However, in the EBM the data of RPUFs tensile properties obtained from experiment were directly fitted by Eq.2.

Fig.4 showed the stress distribution diagram of RPUFs simulated by CSM. It can be seen that the internal stress concentrated on the cellular structure which was perpendicular to the direction of tensile stress. However, the cellular structure region where the stress concentrated decomposed during heat treatment according to the results of TGA. It made the decomposed cellular structure break down more easily and finally accelerated the failure of RPUFs.

Fig.5 showed the stress-strain curves of untreated RPUFs and treated at 200 °C obtained from experiment, CSM and EBM. It can be seen the data obtained from CSM and EBM were agreement with the experimental data. Besides, the acceleration failure effect of stress concentration on cellular structure also can be confirmed by FEA. It can be seen that the tensile strength and modulus obtained from CSM and EBM also decreased after heat treatment. In addition, the tensile strength and modulus obtained from

CSM are more agreement with the experimental values in comparison to those of EBM of RPUFs. The relative difference of tensile strength and modulus values obtained from CSM and experimental measurements was under 2%.

Keywords: rigid polyurethane foams (RPUFs), tensile failure, heat treatment, finite element analysis (FEA)



Fig.1 Experiment setup of tensile specimens

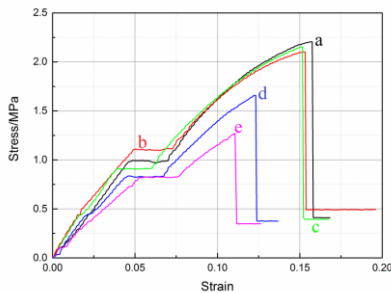


Fig.2

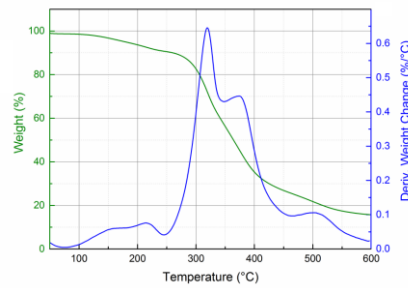


Fig.3

Fig.2 Tensile stress-strain curves of RPUFs: (a) untreated; (b) treated at 50 °C; (c) treated at 100 °C; (d) treated at 150 °C; (e) treated at 200 °C

Fig.3 TG and DTG curves of untreated RPUFs

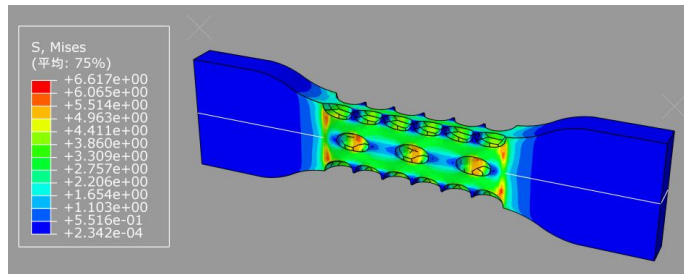
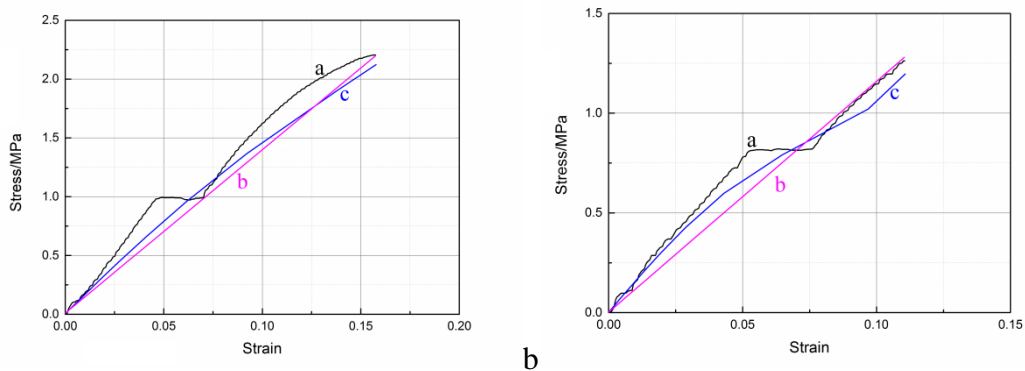


Fig.4 Stress distribution diagram of RPUFs simulated by CSM



a

b

Fig.5 Stress-strain curves of (a) untreated RPUFs and (b) treated at 200 °C obtained from a experiment, b CSM and c EBM

Fracture failure analysis of the outer ring from a grease-lubricated cylindrical roller bearing in an air blower motor

Jiaojiao Xi, Zhiqiang Yu
(Fudan University)
yuzhiqiang@fudan.edu.cn

Abstract: The outer ring of a grease-lubricated cylindrical roller bearing within an air blower motor suddenly failed during operation. The 3D schematic diagram of a cylindrical roller bearing was showed in Fig.1.

In order to identify the causes, diverse characterizations were carried out. Chemical compositions and metallurgical structures of bearing's matrix materials were inspected by photoelectric direct reading spectrometer and metallographic microscope. The results were exhibited the Table 1 and Fig.2, respectively. It was obvious that the carbon content of outer ring, proportional to the steel hardness, was below standard. The chromium exceeded the requirement, while higher chromium could bring about more retained austenite, which were apt to deform under stresses in the microstructure after heat treatment. Thus, it could be concluded that hardness of the outer ring of the failed bearing is intrinsically unqualified. The conclusion also could be supported by the metallographic structures Fig.2a. It was can be seen that more grain boundaries of the retained austenite were present in the outer ring.

Scanning electron microscope was used to detect the microscopic morphologies on the fracture surfaces and contact surfaces. As shown in Fig.3. Typical morphology of quasi-dissociation fracture of dissociation steps along with dimples were presented. Traces of mutual friction and squeeze could be also found on the fracture surface, in Fig.3b, c, respectively, which may have resulted from the contact between the two counterfaces of the outer ring after fracture. Meanwhile, actinomorphous fringes had originated from the corner of the fracture surface. This indicated actually the distinct evidence of the fracture origin.

What's more, the Fourier transform infrared spectroscopy (FTIR) and X-ray diffraction (XRD) were utilized to characterize degradation extent of the greases applied within the roller bearing. The FTIR of fresh and used grease were exhibited in Fig.4. Comparing the results of both, intense carbonyl (C=O) band at 1709 cm^{-1} , that was directly proportional to the degradation degree of grease, occurred in the infrared spectrum of the used grease, indicating oxidative degradation of used greases. The results on XRD of fresh and used grease (Fig.5) revealed that the used grease sample was a complex mixture of compounds like MoS_2 , Cu-Zn intermetallic and FeCr_2O_4 , rather than only MoS_2 in fresh grease, which further verify the oxidative degradation of used greases.

Based on these analytic results, conclusions were put forward that the outer ring of the failed bearing was intrinsically unqualified, and surface of the outer ring of the bearing contained contact fatigue damage. The lubricating grease was subjected to severe thermally induced degradation due to high service temperature, and the lubricant film in the roller/outer ring contacts was not formed effectively. Thus, the interaction between dry friction and impact both led by the degraded grease due to decomposition and oxidation, which resulted in serious wear of the outer ring, was the main cause that originated and propagated the fatigue cracks on the corners of the outer ring, and eventually resulted in the fracture failure of cylindrical roller bearing.

Keywords: fatigue wear, oxidative degradation of greases, fracture failure analysis

Table 1 Chemical compositions of the failed roller bearing (wt%)

Element	C	Si	S	P	Mn	Cr
Outer ring	0.851	0.314	0.007	0.009	0.269	1.751
Roller	0.964	0.583	0.009	0.011	1.064	1.464
GB/T GCr15	0.95-1.05	0.15-0.35	≤0.025	≤0.025	0.25-0.45	1.40-1.65
AISI E52100	0.98-1.10	0.15-0.30	≤0.025	≤0.025	0.25-0.45	1.30-1.60

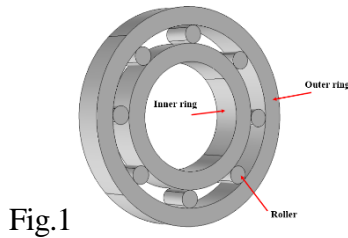


Fig.1

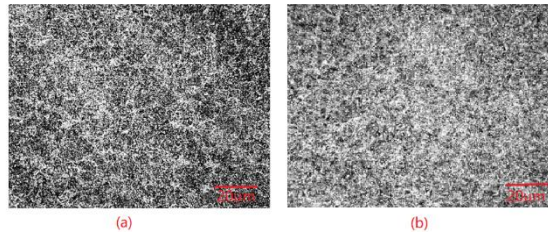


Fig.2

Fig.1 The 3D schematic diagram of a cylindrical roller bearing

Fig.2 Metallographic structures of the failed roller bearing: (a) outer ring, ×500, (b) roller, ×500

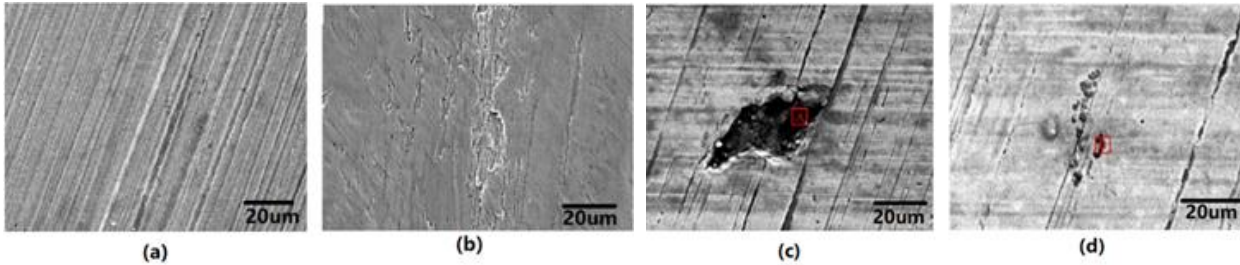


Fig.3 SEM morphologies of the contact surface on the outer ring: (a) normal morphology, (b) irregular trenches, (c) concave, (d) adhered substances

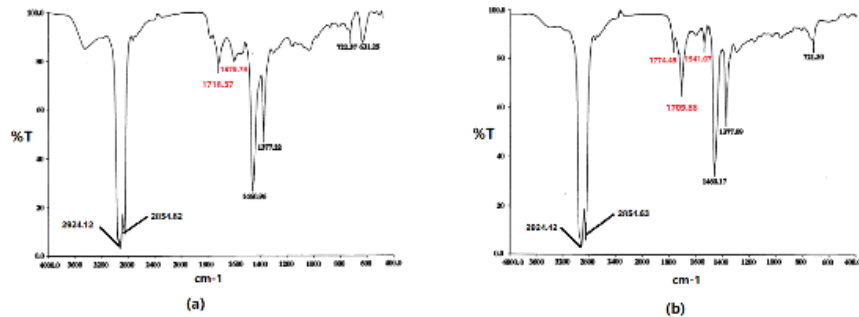


Fig.4 FT-IR spectra of (a) fresh and (b) used grease sample

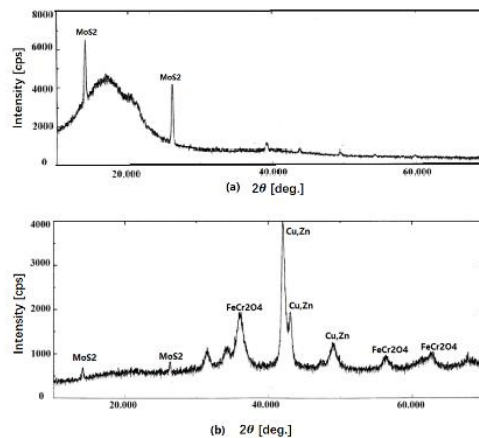


Fig.5 XRD spectra of (a) fresh and (b) used grease sample

Abnormal failure analysis of NiSiCr3552 cast exhaust manifold

Tongwei Ni¹, Yongjun Bian², Zhenguo Yang¹

(1. Department of Materials Science, Fudan University;

2. National Center of Iron and Steel Products Quality Supervision and Inspection Tangshan)

zgyang@fudan.edu.cn

Abstract: Exhaust manifold is an important part of a car. It is mainly used to collect the exhaust from each cylinder of automobile engine and import the exhaust into the exhaust pipe. As the exhaust has high temperature and pressure, the exhaust manifold works under relative complex conditions. Under such conditions, the exhaust manifold may encounter severe failures, causing potential security risks. Therefore, the safety of the exhaust manifold should be paid more attention.

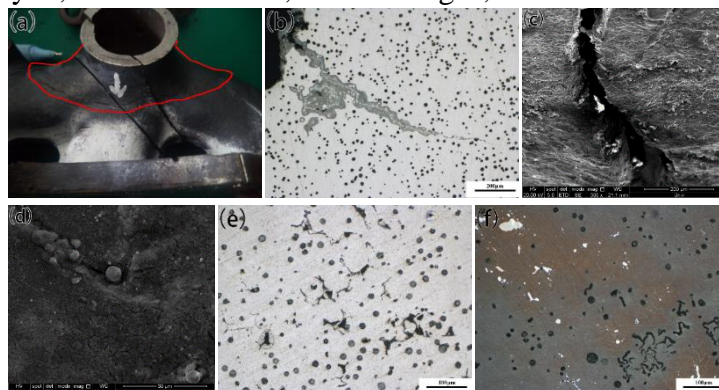
In this paper, the NiSiCr3552 cast exhaust manifold (hereinafter referred as cast exhaust manifold) produced by an auto parts Co., Ltd. was found to crack many times in the 1.5 displacement bench tests. After visual inspection, these cracks was almost near the flange plate, as seen in Fig.1(a). In order to solve this problem, the reinforcing bar had been added to the location of the cracks. However, the cracks was still discovered at the same location. This implied that the cracks of the exhaust manifold was not caused by accidental factors. It must have some inevitable factors which caused the exhaust manifold to crack. Thus it is necessary to study the cracks of the cast exhaust manifold to find out the root reason of failure. It would be helpful to the safe use of the cast exhaust manifold.

For ascertaining the root reason of the failure, material identification, metallographic inspection, hardness test, macro and micro observation of the cracks, and mechanism analysis were carried out. Concretely speaking, material identification and hardness showed that the chemical component and the mechanical property of the cast exhaust manifold was in accordance with the specified requirements. Macro observation found that the cracks initialed from the outside surface of the cast exhaust manifold, as presented in Fig.1(b). Micro observation found that there were fatigue striations and high temperature oxidation particles on the fracture, as displayed by Fig.1(c) and (d). Metallographic inspection around the cracks discovered some cast defects, including inclusions, carbides, and abnormal spheroidization. These defects reduced the local mechanical property and the resistance to high temperature oxidation.

According to the above tests, it could be concluded that the cracks were caused by thermal fatigue, which was related to two factors. On the one part, due to the high temperature gas erosion and the temperature difference, a high temperature stress field around the flange plate was generated. It would lead to high stress around the flange plate. On the other part, the cast defects in the cast exhaust manifold would cause stress concentration. Under the effect of these two factors, the cracks occurred around the flange plate.

Based on the above analysis, some practical countermeasures were proposed to solve corresponding problems. Remove the tempering process to reduce the precipitation of carbides. 1) Raise the pouring temperature to improve the refining process. 2) Increase the cooling rate after normalizing process to avoid the precipitation of the phase with low melting point. 3) Cut down the nickel content to reduce the elemental segregation. 4) Add heat sink to the flange plate to reduce the thermal stress.

Keywords: failure analysis, exhaust manifold, thermal fatigue, cast defects



Fracture failure analysis on the bottom side beam of Q355GNH container

Long Liu, Nan Li, Zhiqiang Luo, Xiaodan Zhang

(Central Laboratory, Central Iron and Steel Research Institute)

liulong@nccast.com

Abstract: The research objects in this paper are fracture failure on the bottom side beam of Q355GNH container. The comprehensive analysis of the fractured bottom side beams of the container were carried out through chemical analysis, mechanical testing, gold phase examination and fracture analysis. The macroscopic results showed that both cracks were at *R* angle of the bottom side beam, cracking along the axial direction, and the thickness of wall was significantly reduced by nearly 50%; the results of chemical composition test showed that Mn content met the demand of Japanese standard, but more than American standard and national standard. Moreover, the chemical composition of the steel plate of 2# crack is analyzed, the results showed that the content of Mn element is more than the deviation of Mn element in the GB/T 222. At the same time, there is little acid soluble aluminum in cracked bottom side beam steel, so it has the high brittleness tendency at room temperature. Mechanical test results showed that strength of the failure parts meet the American standard, Japanese standard, but tensile strength of three quarters of the samples did not meet the requirements of GB/T 4171, tensile strength is beyond the standard limit, the elongation rate of steel plates after breaking is lower than that of American standard, Japanese standard and Chinese national standard. At the same time, the bending performance did not meet the requirements of Japanese standard and national standard. The test results showed that the steel plate of the bottom side beam has high strength and low plasticity. The microanalysis results showed that the inclusion was well controlled, and the normal site of the base structure was upper bainite and granular bainite. The microstructure of the fracture adjacent area was found that the adjacent area was obvious weld structure, indicating that the area was welded. As the existence of welding seam, the toughness of the bottom side beam at the *R* angle will decrease significantly, and it will become the weak link in the process of stress due to its location in the stress concentration. The results of fracture analysis showed that the fracture surfaces of cracks 1# and 2# were dimple fracture, and the macroscopic fracture showed one side of the central depression of the fracture, and the other side matched the morphological characteristics of the central bulge of the fracture, which is in line with the morphological characteristics of the fracture under tensile stress. The *R* angle of the bottom side beam has been welded, so the *R* angle of steel plate may crack during the bending of the roller plate, and the crack is long according to the weld length. However, the content of acid soluble aluminum is very low, which easily leads to high transition temperature of brittleness and toughness of steel plate and causes brittle cracking during bending process. Based on the above analysis results, it can be inferred that the plasticity of material is poor, and the thickness of the steel plate at the *R* angle had thinned nearly 50%, which seriously affected the bearing capacity of the beam under external forces. At the same time because it was welded to lower the area's toughness. In the process of container operation, the container was loaded and acted upon. As the concentrated part of the stress at the *R* angle, it was suddenly broken by the tensile stress

Keywords: bottom side beam, welding line, dimple fracture, tensile stress

New interpretation of materials failure analysis and its application

Zhenguang Yang

(Department of Materials Science, Fudan University, Shanghai 200433)

Abstract: Material failure analysis can not only find the root cause for the failure of structural components by comprehensive analysis so as to avoid reoccurrence of similar accident, but also enhance safety reliability of the structural components by guiding correct ways to develop new materials and modify existing materials. So its engineering value and scientific significance are extremely important. However, the contemporary discipline of the material failure analysis still needs to be improved both from concept or philosophy and from theory or method, to make it be more integral science system and to promote its sustainable development and popularization, so as to attract more people especially young people to participate in the material failure analysis, making their due contributions to nation's economy construction, safety production and social stability.

In this lecture, a new definition of material failure, a new classification of material failure mode, a new formulation of the relationship between material failure mode and failure mechanism and a novel philosophy for ensuring service safety of the structural components were put forward by critical lecturing and exploration based on taking as the carrier the Shanghai top-quality course "material failure analysis", selecting as teaching plans dozens of major engineering failure analysis projects completed in latest five years in ten industries such as nuclear power, thermal power, wind power, petrochemical engineering, chemical engineering, metallurgy, automobile, microelectronics, printed circuit and urban pipeline, and considering as a goal the development of new materials used for failure prevention. Meanwhile, by adopting the proposed case teaching method with seven characteristics, i.e. knowledge, thought, fun, logic, prospective, practicability and interaction, the basic theory, analysis method and engineering application of the material failure analysis were systematically described and illustrated. By means of promoting teaching by research, not only students were attracted to be interested in the material failure analysis and basic knowledge and fundamental theory of the material failure analysis were comprehended, but also students were taught how to utilize the existing fundamental knowledge and analysis method to analyze and solve practical engineering problems. Their innovative abilities, comprehensive capabilities and essential qualities were thus effectively trained and enhanced and teaching objective of unifying trinity among knowledge imparting, ability training and quality education were reached, from which students were greatly benefited and better teaching results were achieved as well. Therefore, the lecture has implications for scientific and technical workers who engage in the material failure analysis and has more useful to staffs who teach course of the material failure analysis.

Keywords: materials failure analysis, top-quality course, new interpretation, case teaching method with seven characteristics

Corrosion failure analysis of 20/316L bimetal-lined pipe under strong acid environment

Wenwen Xiao, Wenguang Zeng, Yuanyuan Zhu, Yanyan Xu, Pengli Ge, Qiuying Gao
(SINOPEC Northwest Oilfield Company)
zhu_yuan20@126.com

Abstract: The bimetal composite pipe is composed of two different materials. It is mainly composed of carbon steel material, which guarantees the strength and toughness of the bimetal tube. Stainless steel and nickel-base alloy and other corrosion-resistant materials are lining tubes, with special method welding or special structural connections at both ends. Due to its excellent mechanical and mechanical properties, good corrosion resistance and relatively low price, it has been widely used. However, with the promotion and application of 20/316L bimetallic tubes in the production of oil and gas, the corrosion failure of the inner liner 316L stainless steel has become more prominent, especially in the harsh environment of acid concentration. In the western oil field, when the 20/316L bimetal-lined pipe was used as the pipeline, collecting the mixture of condensate oil, natural gas and formation water, there is a local corrosion occurred in the inner wall of the inner liner 316L stainless steel. An system analysis on the corrosion failure of 20/316L bimetal-lined pipe was conducted by some advanced measure techniques, for example scanning electronic microscopy (SEM) and energy dispersive spectrometer (EDS), main reasons of failure was defined. Macroscopic observation of 316L lining pipe wall corrosion situation, its surface is black oil, there is a certain amount of the bottom of the pipe with a number of different sizes, shapes and lateral distribution of local corrosion pits, between 0.6 mm to 5.8 mm in length, mainly distributed in the bottom of the pipe body. By microstructure analysis lining tube, 316L stainless steel containing alumina, spherical oxide etc. Nonmetal inclusions, the presence of these inclusions can promote the region of the breakage of the passive film and metal substrate dissolve quickly and cause pitting. Using EDS to analyze corrosion products, the main elements in pitting pits were Fe, Cr, S, O, Mn, Ni and Si. The main elements outside pitting pits are Fe, Si, Cr, Mo, Mn, Ni, and do not contain S elements. There are more S elements in the pitting pit, and the existence of H₂S promotes the formation and development of the pitting pit to some extent. Combined with corrosive environment and production conditions, it is believed that when high concentrations of H₂S and Cl⁻ existed, these areas which were susceptible to the local structural damage to passivation layer and the local dissolution of metal substrate became the sources of pitting corrosion, such as the location of poor passivation layer and nonmetallic inclusions. Ultimately they developed into corrosion pit.

Keywords: 20/316L bimetal-lined pipe, H₂S-Cl⁻, pitting corrosion

Failure analysis of quenching cracking of 45 steel flange

Ce Hao, Huiqiang Wang
(Hebei Agricultural University)
whq@hebau.edu.cn

Abstract: According to cracking of 45 steel vehicle flange after quenching, its observed the microscopic morphology of the fracture and confirmed that the quenching crack of 45 steel vehicle flange is a fracture along the crystal by using scanning electron microscopy(SEM). The fracture along the crystal is brittle fracture. The cause of brittle fracture is the stress concentration at the grain boundary. The stress that can cause cracking must be very strong. The strong stress is produced during the cooling process and that is one of the main reasons for the cracking of 45 steel vehicle flange. The surface hardness of 45 steel vehicle flange is tested by hardness tester. By measurement, getting its surface average hardness that is 55.17 HRC. This is a high hardness number, according to the relationship between quenching hardness and cooling rate of 45 steel, the faster the cooling speed, the higher the surface hardness, so it can be inferred that the cooling rate is too fast during quenching. Non-metallic inclusions have great influence on the properties of materials. Using microscope to observe the metallographic structure finding the non-metallic inclusions were very few, therefore, the material of 45 steel vehicle flange is not the cause of cracking. But there are obvious banded defect groups by observing the micro-structure of the flange after quenching. The banded structure is produced in the process of forging and forming and banded structure is defect prevention. The banded structure greatly reduces the reduction of the area of the material. The reduction rate of area is an important index of material performance. The smaller the reduction rate of area, the greater the brittleness of the material. So the banded structure is an important factor leading to the cracking of 45 steel vehicle flange. In order to prevent the 45 steel vehicle flange from cracking during quenching, banded structures must be eliminated. The quenching risk dimension of 45 steel is 5-12 mm, the thickness of 45 steel vehicle flange is about 8mm. This size is right between the dangerous dimensions, this increases the risk of 45 steel vehicle flange cracking. According to the analysis of observation and test results, the reason for the cracking of 45 steel vehicle flange after quenching is that the flanges have banded structure and the cooling rate is too fast. To prevent 45 steel vehicle flange cracking should to reduce cooling rate and to eliminate the banded structure. The stress is related to the cooling rate, reducing the cooling rate is to reduce stress generation. Normalizing can be used to eliminate banded structure. It proved by experiment that the method of normalizing heat-treatment before quenching and reducing the cooling rate can effectively prevented cracking of 45 steel vehicle flange after quenching.

Keywords: 45 steel, vehicle flange, quenching, failure analysis

Failure analysis of TP92 steel piping

Jeffery Henry

(ATC-Engineering Service)

Abstract: In the mid-1980's a failure in a section of seam welded piping at a US power plant resulted in the death or severe injury of 16 plant workers. The subsequent investigation into the cause of the piping failure made clear that industry experts did not have a complete understanding of the behavior of weldments at elevated temperatures, and this imperfect understanding resulted in the mis-interpretation of key pieces of evidence in the early phases of the failure investigation.

This presentation will review details of the investigation into the Mohave failure and discuss how incorrect assumptions made by investigators regarding the elevated temperature behavior of welds delayed a full understanding of the root cause of the failure.

Keywords: failure analysis, TP92 steel piping

Failure analysis and prevention of heat-resistant alloy tube in petrochemical industry

Tao Chen, Xuedong Chen, Zhibin Ai, Zhichao Fan

(Hefei General Machinery Research Institute Co., Ltd., National Technology Research Center on Pressure Vessel and Pipeline Safety Engineering, China)

Abstract: Heating furnace is the key component of petroleum refining and petrochemical industry, the outer wall of the furnace tube is directly heated by the flame. The medium in the tube is flammable and explosive, and the operating conditions are harsh. In recent years, under the conditions of large-scale and high parameter petrochemical plant, inferior raw material, long period operation, energy saving and environmental protection in Sinopec, there are new changes in service temperature and medium of heat-resistant alloy tubes in heating furnace, and the damage mechanisms and failure modes become more complicated. In this paper, dozens of failure cases of typical heating furnace tubes in large millions of tons of ethylene and ten million tons of oil refining enterprises in China are summarized, the main damage mechanisms (including creep, carburization, stress relaxation cracking, metal dusting, thermal fatigue, molten salt corrosion, stress corrosion cracking, etc) and failure modes (including material deterioration, thinning, bulging and deformation, cracking, etc) of heat-resistant alloy tubes are described emphatically. In view of the main failure reasons of the above furnace tubes, the preventive measures are put forward.

Keywords: heating furnace, tube, damage, failure

Failure analysis of components and fracture mechanisms of metallic materials

Z. F. Zhang, R. T. Qu, Z. Q. Liu

(Materials Fatigue and Fracture Division, Shenyang National Laboratory for Materials Science, Institute of Metal Research, Chinese Academy of Sciences, Shenyang 110016, China)

zhfzhang@imr.ac.cn

Abstract: Fatigue and fracture are two typical failure modes for structural components in service. In this talk, some typical failure cases of components will be given and discussed. Then, based on the analysis of substantial experimental observations of fracture behaviors of metallic glasses and other high-strength materials, here we have developed a new fracture criterion and proved it effective in predicting the critical fracture conditions under complex stress states. The new criterion is not only a unified criterion which unifies the three classic fracture criteria, i.e., the maximum normal stress criterion, the Tresca criterion and the Mohr-Coulomb criterion, but also a universal criterion which has the ability to describe the fracture mechanisms of a variety of different high-strength materials under various external loading conditions. Furthermore, in terms of the universal fracture criterion above, we show that the fracture of metallic glasses originates from the thermodynamic destabilization of the amorphous structure driven by imposed mechanical energy. The fracture behaviors and properties of metallic glasses can be predicted precisely and comprehensively just according to their elastic constants.

Keywords: fatigue failure, fatigue strength, yield strength, tensile strength

Pipeline deformation and monitoring technology

Zheng Zhang, Deli Chen

(Beihang University, Beijing Skyris Technology Co., Ltd.)

Abstract: Pipeline is one of the important transportation channels. The medium transported by pipeline is highly flammable and explosive. The failure of pipelines often leads to catastrophic accidents. It is often associated with the stress of pipeline. The change of the external load makes the pipeline axial tensile stress and bending stress change. Then, the elastic deformation and plastic deformation happens. Through the deformation monitoring in pipeline, the damage risk is inspected in time, so that the catastrophic accidents could be reduced or prevented. The development of IOT technology makes the remote deformation monitoring possible. The strain data of pipeline is collected through strain sensors installed on the surface of pipeline, and transmitted to the data server via mobile telecommunication networks. When the trend and variation of stress exceeded the early warning threshold, the monitoring system would issue an alert automatically. The pipeline safety issue could be found and prevented in advance.

Keywords: pipeline, deformation, monitoring

Failure analysis of the balance ball pin in the car steering system

Ruidong Guo, Song Xue, Ailin Deng

(School of Manufacturing, Southwest University of Science and Technology)

xuesong2004@126.com

Abstract: A balance ball pin used in the car steering system was found broken into two pieces. Macroscopic examinations, scanning electronic microscopy (SEM) examination, metallographic examination, hardness measurement and chemical composition analysis have been made to figure out the main failure reason. The results indicated that fatigue fracture is the main fracture mode, and the unreasonable surface quenching resulted in inhomogeneous thickness of quench-hardened case. As a result, micro cracks along the circumferential direction emerged on the subsurface of the quench-hardened case. Moreover, in the working of the ball pin, the stable rod didn't turn smoothly and fitting surface was worn badly, where produced the large resistance, which is the main torque to the ball pin.

Keywords: failure analysis, balance ball pin, micro cracks, fatigue fracture

Failure analysis of an automotive bushing

Ailin Deng, Song Xue, Ruidong Guo

(School of Manufacturing, Southwest University of Science and Technology)

xuesong2004@126.com

Abstract: The reason of the longitudinal fracture of automotive bushing during the assembly process is presented in this study. On the basis of macroscopic inspection, scanning electron microscopy (SEM), energy dispersive spectroscopy (EDS), microstructural examination, chemical analysis and hardness measurement, the fractography investigation indicates that cleavage fracture is the dominant fracture mode, and the fracture near the outer surface of bushing is covered by impurity substance which is similar to the composition of the coating. Therefore, it is possible to infer that the crack has existed before installing. In addition, the detailed metallurgical analysis demonstrates decarburization at the fracture surface which causes folding defect. In the process of assembly of bushing, the stress concentration and surface defect promote the old crack initiation and propagation, finally, lead to the fracture of the bushing.

Keywords: failure analysis, bushing, cleavage fracture, folding defect

Study the cases of the cracking failure of automobile steering knuckle

Weilian Sun
(Hebei Agricultural University)
sunweilian@hebau.edu.cn

Abstract: The cracking of the automobile steering knuckle and shaft that were made of 40Cr alloy steel of quenching and tempering treatment occurs during use. Through the research on microstructure, non-metallic inclusions, hardness and chemical composition of these two kinds of cracked automobile steering knuckle and shaft after heat treatment, these devices are used such as metallographic microscope, rockwell hardness tester, micro hardness tester, scanning electron microscopy, energy dispersive spectrometer and so on. There have some heat treatment defects of segregation ferrite and troostite in the microstructure, at the same time, the chemical composition and microstructure were observed by electron microscopy, the main reasons for the cracking of steering knuckle and shaft were analyzed, these can provide improvement opinions for the specifications of the quality inspection of the automobile steering knuckles and shaft parts in the future.

Keywords: automobile steering knuckle, quenching and tempering treatment, ferrite, troostite

Failure analysis on leaked titanium tubes for seawater heat exchanger in recirculating cooling water system of coastal nuclear power plant

Yi Gong, Zhenguo Yang
(Department of Materials Science, Fudan University)

Abstract: Thanks to the superior resistance to degradation, especially the chloride-induced pitting corrosion, titanium and its alloys are commonly ideal for application in the seawater environment. However in this paper, one failure case regarding leakage on the titanium tubes of the seawater heat exchanger in the recirculating cooling water system of one coastal nuclear power plant in China was addressed. Actually, this problem with severer extent on even a larger number of tubes had already occurred and been effectively solved before, however this time it came out again but merely affected several individual tubes. To avoid contamination of the moderator system, plugs were temporarily adopted for the leaked tubes, but undoubtedly root cause analysis of this failure was immediately necessitated to reduce both the safety risks and the economic losses. Hence, systematic investigation of the base materials, environmental media, defect morphologies and micro-area compositions etc. were carried out for identification of the failure causes, then based on which the relevant mechanisms were discussed and the pertinent countermeasures were proposed. Achievement of this paper will not only help to solve the practical engineering problem for this nuclear component, but also lead to a better understanding from the materials science point of view for the titanium alloys under complex service conditions.

Keywords: titanium tubes; heat exchanger; nuclear power plant; seawater; failure analysis; erosion and corrosion

Design and test analysis of bionic subsoiler tip

Jianyong Guo, Qingda Li, Jun Hu
(Heilongjiang Bayi Agriculture University)
liqingda23@126.com

Abstract: The subsoiler tip has a great deal of wear due to long-term directly contact with the soil. Based on the viewpoint of bionics, this paper develops a bionic subsoiler tip. It takes the mid-toe of the mouse's front paw as a biological model, and selects the nodular cast iron with good toughness and wear resistance. In order to accurately obtain the stress distribution of the subsoiler tip in working conditions and provide a theoretical basis for wear resistance treatment, this paper uses the Workbench module in ANSYS to perform static analysis on the subsoiler tip to obtain the stress distribution map. From the stress distribution diagram, it can be concluded that the stress of the subsoiler tip is mainly concentrated in the middle region, so wear and tear in this region is the fastest. Through the field wear test, the results of the finite element analysis can be verified. It is proved that the wear rate of the middle region of the subsoiler tip is the fastest. When using surface welding, surface cladding and other methods for wear-resisting treatment, it can be targeted to strengthen the easy-to-wear region of the subsoiler tip to greatly save material consumption and avoid material waste.

Keywords: subsoiler tip, wear, bionic, finite element analysis

Investigation on typical failure mode of high-pressure hydrogen

storage tanks for vehicles

Yiwen Yuan, Yannan Du, Bo Yang
(Shanghai Institute of Special Equipment Inspection and Technical Research)
yuanyw@ssei.cn

Abstract: Cylinder with an aluminum liner for storage of compressed hydrogen gas as a fuel for vehicles is currently the main international energy storage container for hydrogen fuel cell vehicles, which has the advantages such as light weight, high pressure resistance and so on. Such cylinders filled with hydrogen gas are generally pressurized to 35-92 Mpa. Therefore, the failure of the cylinder may have a vital impact on life and property. Through a series of comparative experiments, the typical failure mode of such hydrogen cylinder is summarized as follows. It mainly includes irreversible failure, recoverable failure and preventable failure. Irreversible failure mainly refers to the failure mode such as leakage, rupture and penetration, etc., which could make the cylinder not restore its original function. Recoverable failure mainly includes thread damage, security attachment startup and so on. The original function of the cylinder could be repaired by repairing the thread and replacing the safety accessories. Conditions such as load at extreme ambient temperature for a long time, filament wound layer cracking caused by surface damage, chemical corrosion, serious impact could decrease the cylinder strength, which could belong to preventable failure. The service life could be prolonged by monitoring use process.

Keywords: failure mode, hydrogen storage tank, irreversible failure, recoverable failure, preventable failure

Failure analysis of regenerative gas electric heater outer wall cracking

Bo Zhao¹, Jing Guo¹, Bo Wang², Yuxin Yu¹, Tong Xu¹, Yuhong Xing²

(1. China Special Equipment Inspection and Research Institute;

2. SINOPEC Shijiazhuang Refining & Chemical Company)

zhaobo19840626@163.com

Abstract: Failure analysis in the leakage of a regenerative gas electric heater was founded on October 15th, 2017. The heater was operated in S-Zorb device and total operating time is 200-300 hours. This article analyzed the reason of it with macromorphology, chemical composition, metallography, hardness and fracture morphology, and the equipment design files were also analyzed simultaneously.

The results showed that the failure position presents the thin lip cracking on apparent morphology, and a large amount of mill scale could be seen on the surface of it. Metallurgical structure mainly consisted only ferritic structures instead of ferrite and pearlite structures, and the grains grew up significantly. The results of micro Vickers hardness measurement (HV1) also illustrate this point, and this phenomenon occurred both on the leak spots and other heated surfaces. Chemical composition showed that the content of carbon considerably lower than the requirement of ASME standard and other elements met it.

According to the heater's working condition, it can be considered that unreasonable position design of temperature sensor and defects of equipment structure led to the overtemperature environment on heater outer wall, and caused decarburization behavior of it. It caused the degradation of mechanical properties at high temperature after a period of time, and caused plastic instability fracture.

Keywords: failure analysis, electric heater, decarburization

The influence of copper on the stress corrosion cracking of 304 stainless steel

Xuehan Wang, Chengshuang Zhou, Zhile yang, Lin Zhang

(Zhejiang University of Technology)

zhoucs@zjut.edu.cn

Abstract: An anti-burning boiler happened water leakage from hot water pipe made of 304 stainless steel after it only used 8 mouths. Detection found that 304 austenitic stainless steel in combustion chamber cracked on the side of the hot water outflow. This study analyzed why 304 austenitic stainless steel hot water pipe cracked by the methods like chemical analysis, microstructure test, intergranular corrosion and corrosion product analysis. The results showed that the material of 304 stainless steel was qualified. The fracture was a mixed crack including transgranular crack and intergranular crack (main of transgranular crack). A large number of single copper accumulated on the crack surface. Thus it revealed that the crack of 304 stainless steel is a stress corrosion cracking (SCC) caused by copper ions and mechanical stress. High temperature is another factor induced cracking since passive film of 304 stainless steel weakened in hot water. The copper ions came from inferior copper valves when inferior copper valves immersed in hot water including oxygen. Based on above analysis, the replacement of the hot water pipe to 2205 stainless steel can prevent this cracking. So the stress corrosion behavior of 304 stainless steel and 2205 duplex stainless steel in aqueous solution with a certain concentration of copper and copper chloride were compared and analyzed by using four-point bending test. It found that 2205 duplex stainless steel did not crack while 304 austenitic stainless failed in the test.

Keywords: 304 stainless steel, copper, hot water pipe, stress corrosion cracking, anti-burning boiler

Influence of working temperature on the service behavior of tubing in water injection wells

Lijuan Zhu, Chun Feng, Caihong Lu, Long Jiang, Hang Wang

(State Key Lab for Performance and Structure Safety of Petroleum Tubular Goods and Equipment
Materials, Tubular Goods Research Institute of China National Petroleum Corporation)

zhulijuan1986@cnpc.com.cn

Abstract: Serious corrosion occurred on the tubing with an inner coating used in the lower part of the water injection wells. Measurements and inspection were performed on the chemical composition and metallographic structure of the tubing. The morphology and composition of the corrosion products were characterized by scanning electron microscopy (SEM), energy-dispersive spectroscopy (EDS) and X-ray power diffraction (XRD). The results indicated that the tubing with an inner coating showed good resistance at the temperature of 37 °C and 82 °C; however, local blisters and large areas of blisters of the tubing inner coatings occurred at the temperature of 59 °C and 104 °C respectively. The large areas coating failure was mainly attributed to the poor thermal aging resistance; while the local blisters of the coating was caused by coating defects. The corrosive media penetrated into the poor protective coatings and researched the interface between the coating and the N80 substrate, therefore the N80 carbon steel tubing was largely corrupted. The corrosion mechanisms were mainly corrosion induced by dissolved oxygen and CO₂, Cl⁻, iron bacteria and saprophytic bacteria accelerated the corrosion of tubing to some extent.

Keywords: working temperature, coatings, corrosion, water injection wells, tubing

Analysis and improvement of the cracking cause of the 50CrVA steel stabilizer rod of an automobile

Bo Sun

(Hebei Agricultural University)

48083040@qq.com

Abstract: In the heat treatment process of quenching and tempering, cracking phenomenon was found in the automobile stabilizer rod made of 50CrVA steel. The conventional failure analysis methods, such as component analysis, metallographic analysis and hardness test, only found that the inclusions in the material were slightly exceeding the standard. Local defects were found through sectional examination of the crack morphology by electron microscope. By means of the electron microscope energy spectrum component identification and microhardness test, composition segregation problem was found in the materials. By improving the technology, material waste and major accidents were avoided.

Keywords: 50CrVA steel, automobile stabilizer rod

Fatigue failure of a horizontal tail's hollow shaft of an aircraft—the impacts of surface integrity and stress concentration

Youli Zhu, Shuai Hou, Xiaokun Du, Yongheng Ni
(Armored Forces Institute of the Army)
zhuyl2011@sina.com

Abstract: The failure of a used horizontal tail's hollow shaft of an aircraft was analyzed. Microstructural analysis and hardness measurements showed no degradation of the shaft's material. Morphology observation and roughness measurement showed remarkable inner surface machining marks. SEM and EDS analyses revealed intergranular cracking due to grain boundary oxidation of the inner surface. Fractography of the fracture surface showed beach marks and striations, indicating fatigue as the mode of fracture. Stress analyses illustrated structural stress concentration at the inner fillet and local stress concentration owing to the machining marks. Recommendations were made for improving the fatigue performance of the hollow shaft in manufacturing and maintenance.

Keywords: hollow shaft, fatigue failure, stress concentration, surface integrity

Design and test analysis of bionic subsoiler tip

Qingda Li, Jianyong Guo, Jun Hu
(College of Engineering, Heilongjiang Bayi Agricultural University)
liqingda23@126.com

Abstract: The subsoiler tip has a great deal of wear due to long-term directly contact with the soil. Based on the viewpoint of bionics, this paper develops a bionic subsoiler tip. It takes the mid-toe of the mouse's front paw as a biological model, and selects the nodular cast iron with good toughness and wear resistance. In order to accurately obtain the stress distribution of the subsoiler tip in working conditions and provide a theoretical basis for wear resistance treatment, this paper uses the Workbench module in ANSYS to perform static analysis on the subsoiler tip to obtain the stress distribution map. From the stress distribution diagram, it can be concluded that the stress of the subsoiler tip is mainly concentrated in the middle region, so wear and tear in this region is the fastest. Through the field wear test, the results of the finite element analysis can be verified. It is proved that the wear rate of the middle region of the subsoiler tip is the fastest. When using surface welding, surface cladding and other methods for wear-resisting treatment, it can be targeted to strengthen the easy-to-wear region of the subsoiler tip to greatly save material consumption and avoid material waste.

Keywords: subsoiler tip, wear, bionic, finite element analysis

Failure analysis of a brass valve

Sining Fan, Kaishu Guan

(East China University of Science and Technology)

guankaishu@126.com

Abstract: The aim of this work was to reveal the failure mechanism of a brass valve after 11 years of service in compressed air cylinders. The characterization methods included chemical composition analysis, metallographic inspection, mechanical analysis, scanning electron microscopy (SEM) equipped with energy dispersive spectroscopy (EDS) and hardness test. It can be observed by optical microscope (OM) that cracks were sharp and initiated from the root of internal thread of the valve and. According to the FEM analysis results, stress concentration that was the stress condition for the stress corrosion cracking (SCC) occurred in the root of inter thread. In addition, SEM revealed that fracture morphology was intergranular and a plenty of corrosion productions existed in fracture. These experiments resulted to the conclusion that some factors associated with SCC.

Keywords: valve, failure analysis, stress corrosion cracking, brass

Three fatigue failure analysis of gas cylinder for long tube trailer

Jianming Zhai, Tong Xu, Baolan Gu, Ke Bo, Yonghui Sun, Haiyang Yu

(China Special Equipment Inspection and Research Institute)

jmzhai@163.com

Abstract: Three cylinders of long tube trailer were leaked during the inspection and the type test. In order to analysis the cause of failure, the failure analysis was carried out in this work. The macroscopic observation, metallographic analysis and fracture analysis were used in this research, and the fatigue fracture morphology was found at the fracture sites of all three cylinders. As a result, cylinder 1 was found leaked in the inspection process. The crack is from inner surface to outer surface of the wall, and stripes scratches is found on the inner surface. The metallographic analysis proved that the fatigue crack was originated from scratches in cylinder 1. The scratches caused by the process of machining were sensitive to stress concentration, which made the fatigue crack occur. Cylinder 2 and Cylinder 3 are composite material winding cylinders, and were found failure during the type test, with life of around 13000 cycles. In the metallographic analysis, it is found that the inner surface had many folds in cylinder 2, and the fatigue crack was grown from these folds. The crack of cylinders 3 was found in the position of cylinder bottle shoulder. The original crack which may be caused by spinning process of the bottle shoulder was observed in the fracture analysis, and expanded gradually under the action of cyclic load. These three fatigue failure analysis shows that the quality examination is very important during the process of cylinder production.

Keywords: fatigue failure, fracture analysis, long tube trailer, gas cylinder, process defects

Failure analysis on fractured carbon dioxide fracturing tube

Jiangang Wang

(Hebei University of Science and Technology)

wm094212@163.com

Abstract: An in-service fracture failure of deflation head of airdox occurred in blasting process. Samples from fractured parts were brought for a failure analysis investigation. Fractographic examination and metallographic observation showed that it exceeded tensile strength of the end of component thread because the stress concentration in blasting process. The finite element analysis indicated that the stress state was improved by optimizing the dimensions of the air-bleed hole or circular cone of drill.

Keywords: blasting cartridge, fracture failure, finite element analysis, stress

Metallographic automatic rating technology and its application through machine learning

Li Zhang

(Guangdong University of Technology)

996422291@qq.com

Abstract: metallic materials play an important role in industrial production because of their good process performance and performance. Metallographic analysis is the simplest and cheapest method for analyzing its performance. Metal material classification at present is mainly rely on manual with the help of image processing software to get after the image processing, contrast with the standard image to judge the level of material, this method is inefficient and requiring inspectors have corresponding professional knowledge. In order to improve the efficiency and accuracy of automatic rating prediction for metal materials, this paper proposes a machine learning algorithm applied to the classification of metal materials. Using principal component analysis (PCA), the method of multiple influencing factors of metal material performance dimension, avoid dimension disaster, select important characteristic factors in training, validation and testing. Machine learning algorithms in many ways suitable for the application of multiple classification, this paper respectively using k- nearest neighbor, support vector , artificial neural network (simple three-layer neural network) method such as the hand writing (data set from the MINIST data set, the sample of 60000 copies) are identified. The accuracy was high (>97%).The neural network has high potential, and the simple neural network model can achieve 98.9% accuracy. Similarly, the recognition of metallographic tissue can be identified by using such machine learning methods. Experimental steps: first, preprocessing the acquired image, isolate the tissue that needs to be detected, reduce the complexity of image recognition, and then select the algorithm for training and detection. Conclusion: because the above algorithms have a good robustness, the algorithm suitable for hand writing is also applicable to the project identified by metallographic organization, which can effectively carry out metallographic hierarchy identification.

Keywords: machine learning, neural networks, support vector machine, k-nearest neighbor algorithm

Pipeline failure analysis of phenol acetone

Huigu Yang¹, Sulan Gu², Xiangsen Bu³

(1. Shanghai Institute of Special Equipment and Technical Research; 2. Shanghai Baosteel Inspection Crop;
3. Shanghai Gaoqiao Petrochemical Engineering & Construction Co., Ltd.)

yanghg@ssei.cn

Abstract: It was found that leakage of some places on the pipeline of phenol acetone unit when the device was in trial-operation in December of 2004. The main leakage reason of pipelines is determined that dot-corrosion produced by chlorine hydronium with sample test and analysis such as chemical composition, mechanical properties macro-appearance, metallographic examination, micro-appearance and corrosion-production, etc. It is considered a kind of available method to avoid accumulation of chlorine hydronium for resolve of pipeline failure.

Keywords: pipeline failure, leakage, dot-corrosion

Failure analysis of drill pipe's rotary shouldered thread connection

Fangpo Li

(CNPC Tubular Goods Research Institute)

lifangpo@cnpc.com.cn

Abstract: In this paper, the failure process and mechanism of the drill pipe's tool joint is studied by means of full-scale make-up and break-out (M&B) test. The results show that galling failure of tool joint mainly take place on the position of the leading flank, bearing flank and make-up shoulder of rotary shouldered thread connection. The galling failure of the three different parts is a process of mutual independence and mutual promotion. They may appear simultaneously, and may also appear at different stage. Tool joint's galling failure is mainly due to the plastic deformation and peeling under the effect of compressive stress caused by friction and compression effect among the metal surface in contact. During M&B test, deformation and spalling of metal accumulates continually in the process of movement, and results in "cold welding" forming on local position. In the subsequent M&B process, "cold welding" metal is torn open and peeled off from metal matrix, and galling is getting serious gradually. M&B test result show that torque and thread compound has decisive influence on galling failure, while the influence of threaded connection's surface wear, rearranging, torque fluctuations and tensile load is not obvious.

Keywords: failure and prevention, galling failure, tool joint, M&B test, rotary shouldered thread connection

The countermeasures of failure risk on strength performance of closing part for steel gate valve

Minghai Fu, Yiwen Yuan, Yuqing Yang, Yannan Du
(Shanghai Institute of Special Equipment Inspection and Technical Research)
fumh@ssei.cn

Abstract: Steel gate valves are widely used in petroleum, petrochemical, and power systems. The combination of wedges and stems is called a steel gate valve closing part. Since the closing part is usually opened or closed fully while actual operating, the “blocked” phenomenon may occur if the gate valve which is closed for a long period of time needs to be opened. The ‘blocked’ phenomenon is caused by long-term unusing. If strong opening is used, there is a risk of breaking the closing part. If the breakpoint of valve stem is located inside the valve body, it is an undetectable failure from outside. This illusion that the valve is in good condition will result in an accident. In order to verify the rationality of closing part design, the correctness of the manufacturing process, and the reliability of the product function, a type test is performed for strength of the closing part according to the TSG D7002-2006 specification. By verifying failure risk of the valve closing parts in the test process, failure conditions are explained specifically, and improvement measures and risk countermeasures are proposed.

Keywords: gate valve, closing part, strength, failure, type test

Effects of TiN coating on the very high cycle fatigue properties of

Ti-6Al-4V titanium alloy

Kaiju Lu, Li Cheng, Jingyuan Liu
(Air Force Engineering University)
1104743297@qq.com

Abstract: The application of TiN coating can improve the erosion resistance of compressor blades of helicopter engines significantly. However, it may do harm to the fatigue performance of blades. In this study, three-point bending fatigue testing of Ti-6Al-4V base specimens and coated specimens with three different thickness (5, 15, 25 μ m) were carried out with a 20 kHz ultrasonic testing machine. Results indicated that the duplex S-N curve showed a bilinear decreasing trend. TiN coated specimens had reduced fatigue strength of Ti-6Al-4V specimens, and the thicker the coating is, the more obviously the decrease is. SEM observations showed that with the decrease of the maximum stress, the fatigue crack initiation translated from the surface to the interior of specimens. The defects, such as voids and inclusions in the TiN coating, were prone to form stress concentration and resulted in crack initiations. It was founded that the lamination occurred in the interface between TiN coating and Ti-6Al-4V base material under the higher stress due to the huge difference of elastic modulus.

Keywords: Ti-6Al-4V titanium alloy, TiN coating, three-point-bending fatigue, VHCF

Failure analysis on the cracking of girth weld joint of steam pipeline

Ming Song, Tong Xu, Haiyang Yu Chao Sun, Chao Sun
(China Special Equipment Inspection and Research Institute)
songm214@foxmail.com

Abstract: 12Cr1MoV is a commonly used heat-resistant steel in the steam pipelines of subcritical power boilers in China. Usually, the girth weld joints are the weakest areas of the entire steam pipeline. In this work, a failure case about the leakage of 12Cr1MoV steam pipe girth weld joint, which had served for about 10 years, was analyzed. The marco-fractography showed the non-ductility cracking along the hoop direction, and the crack plane complete duplicating the morphology of the fusion line. The microstructure observation illustrated the cracks are all located at the grain boundaries of the intercritical heat affect zone. Creep cavities were also observed along the grain boundaries. These phenomen suggest the failure of the weld joint is type IV creep cracking. According to the 180 °cracking along the hoop, the weld joint might have suffered an abnormal bending moment during service, which should be the root cause of the early time creep cracking.

Keywords: type IV creep cracking, steam pipeline, girth weld joints, 12Cr1MoV

Failure analysis on energy conservation equipment in waste heat boiler system

Shenghui Wang¹, Chenhuai Tang¹, Gong Yi², Qun Ding³, Zhenguo Yang³
(1. hanghai Institute of Special Equipment Inspection and Technical Research;
2. Department of Materials Science, Fudan University; 3. Materials Science, Fudan University)
wangwish6@163.com

Abstract: Waste heat boiler system is primarily used to deal with waste water produced in upstream plants. The failed equipment discussed in this paper are evaporator and economizer. The support plates of evaporator and elbows of economizer suffered from severe corrosion. The medium of evaporator and economizer are exactly the same. The tube side is water, the shell side is hot exhaust gas. Sulfur element is detected from corrosion products of two equipments. But different failure mechanism are found. In order to find out the root cause of failures, material examination, macro/microscopic observation and chemical analysis are conducted. Failure mechanism of the two material are discussed. It is determined that the high-temperature oxidation resulting from short-time overheating is the root cause of the plate failure. The failure mechanism of elbows is found to be sulfuric dew point corrosion. Finally, corresponding countermeasures are suggested.

Keywords: support plate, evaporator, high-temperature oxidation, elbow, economizer, dew point corrosion

Failure analysis of 45 steel hydraulic cylinder ear

Huiqiang Wang
(Hebei Agricultural University)
317395437@qq.com

Abstract: Hydraulic brick making machine is a machine that producing high-strength cement brick, hollow block or Color brick road brick through scientific ratio, water mixing and hydraulic press, using bira nest, cinder, fly ash, stone powder, sand, gravel, cement as raw materials. As a new alternative clay brick equipment, hydraulic brick machine that can produce a variety of models of new wall products through the replacement of the mold has functions of environmental protection, energy saving, hydraulic, electronic control, mechanotronics. 45 steel is high-quality carbon structural steel, whose hardness is not high. It can be cut easily and shows a good comprehensive mechanical properties after quenched and tempered. Thus it is widely used in various types of important structural parts, especially those connecting rods, hooks, bolts, gears and shafts working under alternating load. The hydraulic cylinder is the main force and power support element of the construction machinery, and the movement of the mechanism is achieved by the extension and retraction of the hydraulic cylinder piston rod. The force parts of a hydraulic cylinder often fail because of the host vibration or oscillation. Meanwhile, the hydraulic cylinder is subjected to a great deal of internal pressure up to 40 MPa or even much higher. Higher demands are required for the structure of the hydraulic cylinder to adapt to the complex force conditions, especially the hydraulic cylinder earrings, which have a higher safety requirements as the main force parts and movement support parts. The working position of hydraulic cylinder earrings in the hydraulic brick machine is given in Fig.1(a). The macroscopic morphology of the broken hydraulic cylinder earrings are shown in Fig.1(b). The morphology of sample cut from the fracture of the earring with a special cutting machine and cleaned with an SB-5200D ultrasonic cleaner was shown in Fig.1(c). This paper investigates the failure of an ear on a hydraulic cylinder. The hydraulic cylinder ear on a hydraulic brick making machine produced by a factory was soon cracked during running. The fracture morphology, chemical composition, microstructure and hardness of 45 steel failure ear were analyzed by using of scanning electron microscopy, energy spectrometer, direct reading spectrometer, optical microscope and microhardness tester. The results showed that more Al_2O_3 and sulfide non-metallic inclusions in the fracture section, the defects microstructure were net ferrite and pearlite, the inside were exist obvious band microstructure and widmanstatten structure, the local coarse grain were the main reason cause the failure of hydraulic cylinder ear.

Keywords: hydraulic cylinder ear, 45 steel, non-metallic inclusions, widmanstatten structure



Fig.1 Macromorphologies of the fracturing hydraulic cylinder ear: (a)working position of ear; (b)fracture of ear; (c)morphology of fracture

Mechanism of fault slippage and influence on casing deformation for horizontal shale gas wells

Xueli Guo¹, Jun Li¹, Gonghui Liu², Yan Xi¹

(1. China University of Petroleum; 2. Beijing University of Technology)

clouder0713@163.com

Abstract: The multi-stage hydro-fracturing of horizontal wells has become an effective technology for shale gas reservoirs. Whereas, casing deformation problems occurred severely during the fracturing processes. Through statistical analysis, natural faults distributed at multiple length scales system around the casing deformation points. During the multi-fracturing operation, the pore pressure and the displacement of formation would be large enough to reactivate the natural faults, causing faults slippage then leading to casing deformation. A two-dimensional model considering entire formation mechanics system of faults and surrounding shale rock was established to study the fault slip path. The slipping mechanism was analyzed from the perspective of solid quasi-static methods. Mohr-Columb criterion was used to evaluate the possibility of faults slippage under the condition of excess pore pressure. Besides, the characteristic of micro-seismic signals, such as the geometrical shape, magnitude anomaly signal, and b-value of the magnitude-frequency formula, was also used to judge the fault slippage during fracturing. The fault slip distance was calculated based on the principle of the focal mechanism. Then a three-dimensional casing-cement sheath-formation finite element model considering transient thermal-pressure coupling effect was established to reveal the influence of fault slippage on casing deformation failure. The finite element model considered the whole process of drilling, casing, cementing and fracturing, which was called the stage finite element model procedure. This procedure includes four parts: Pre-stressing, simulating the state before drilling. The initial geo-stress are loaded in the model through the predefined field. Drilling, the elements representing these rock are removed through the keywords of Model change. Casing, cementing, and Fracturing. Sensitivity analysis was carried out for different faults radius. From the above analysis, some conclusions can be drawn:

- 1) The stiffness ratio between formation and fault had great influence on fault slippage. When the stiffness ratio is less than 1, the fault could be easy to slip. The slippage occurred at the displacement turning point, indicating that the instability was the extremum of the displacement form. The stress on the fault surface jumped suddenly.
- 2) When the pore pressure of the fault reaches or exceeds the critical pore pressure or the micro-seismic distribution is skewed with the borehole, or the b-value in the G-R formula is less than 1, or the signal intensity is abnormal, the fault is sliding. The smaller of b, the more severely the fault slips.

Keywords: fault stability path, casing deformation failure, fault slippage, micro-seismic, focal mechanism, shale gas fracturing

Evaluation of irradiation degradation of nuclear cable materials by the infrared microscope approach

Gong Yi¹, Jie Tang¹, Xiaolei Yang¹, Zhenguo Yang¹, Xiuqiang Shi², Yongcheng Xie²,
Aihua Guo³, Jianfeng Xu³

(1. Fudan University; 2. Shanghai Nuclear Engineering Research & Design Institute Co., Ltd.;
3. Shanghai Institute of Process Automation Instrumentation Co., Ltd.)
zgyang@fudan.edu.cn

Abstract: To predict the lifetime under normal service conditions and to ensure the safety under postulated accidental conditions for the electrical equipment like cables in nuclear power plants, accelerated ageing testing is compulsory in equipment qualification to evaluate the degradation behaviors of them that are exposed to the stressors as temperature, pressure, humidity, chemicals, vibration, and especially the characteristic one, irradiation. Actually, it's well known that irradiation degradation depends on diverse factors, and among them the effects of irradiation types and dose rates are the priority concerns. For investigation of these topics, abundant researches have been conducted on nuclear cables and the polymeric materials used for their insulations and sheaths. However, on one hand, most of them were tested from the gamma (γ) irradiation because of the convenient access to the radioactive sources like ⁶⁰Co and ¹³⁷Cs etc., while hardly were emphases laid on the beta (β) irradiation owing to the high cost of the electron accelerators. This fact finally results in the compromising approach that the required beta doses are equivalently (1:1) converted to the gamma doses in the irradiation qualification testing for the nuclear cables. On the other hand, the dose rate effect is always interpreted as the rule 'the lower dose rate, the severer degradation' due to the effect of diffusion limited oxidation. Regardless of its scientific reasonability, it at least makes the time- and cost-saving qualification of nuclear cables impossible in nuclear engineering. Besides of these two issues, another problem is that the materials previously studied abroad are commonly the commercial products with patented formulations, whose universal applicability yet remains in doubt. That is to say, these results are product-specific, making it obliged to evaluate the irradiation degradation behaviors of every 'new' polymeric material prior to its adoption for the nuclear cables, though it is a common one like EPR (ethylene-propylene rubber), EVA (ethylenevinyl acetate), XLPO (cross-linked polyolefin) and so on.

Under this context, in order to comprehensively deal with such issues and to meet the demand for domestication of the polymeric materials for the nuclear cables of the advanced pressurized water reactors in China, irradiation testing that takes into consideration of both irradiation types and dose rates were carried out on the domestically manufactured nuclear cable materials in this paper. Particularly, in addition to the conventional methods grounded on the mechanical and the electrical properties measurement, infrared microscope – the advanced detection technique for chemical property from the microscopic point of view was used. By means of it, the functional groups of interest, e.g. carbonyl, carboxyl, hydroxyl etc. can be directly detected in the precision of micrometers on the whole cross sections of the tested polymeric materials, which therefore makes quantitative investigation of the penetration depth of irradiation degradation possible. The results indicated that the degradation from both gamma and beta irradiation with constant dose rates but varying absorbed doses is similar upon the vinyl-based polymers if taking the elongation at break as the index, seen in Fig.1(a), which therefore verifies the reasonability of the equivalent conversion from absorbed beta doses to gamma doses in qualification testing of nuclear equipment. Meanwhile, the oxidation penetration depth was found obey nearly an exponential decay relation with the thickness away from the surface, as displayed in Fig.2(a). While for the dose rate effect on the same materials, the severest degradation was found occur at the intermediate dose rate instead of the lowest one due to the competing mechanisms between plasticizers volatilization

and chain scission, seen in Fig.1(b). But the oxidation penetration depth was discovered indeed increase with the decrease of the dose rates, and even obey roughly a arithmetic progression relation, as revealed in Fig.2(b), from which the conventional concept that the degradation extent is inversely proportional to the dose rates is testified.

Achievement of this paper would provide a practical approach to evaluate the effect of irradiation degradation on nuclear equipment, and would also lead to a better understanding of the correlation among irradiation types, absorbed doses, dose rates, degradation trend, oxidation penetration depth and degradation mechanisms of nuclear cable materials.

Keywords: gamma irradiation, beta irradiation, dose rate effect, vinyl-based polymers, nuclear cables, carbonyl index, infrared microscope

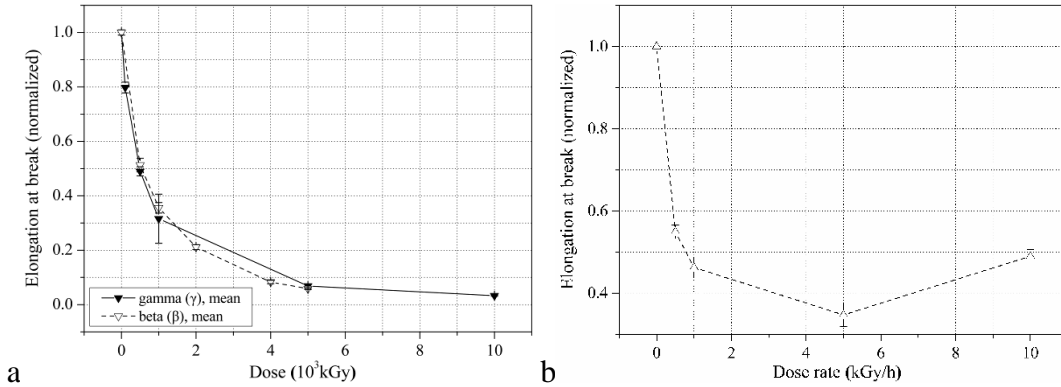


Fig.1 Elongation at break versus (a) absorbed doses from different irradiation types, (b) different dose rates

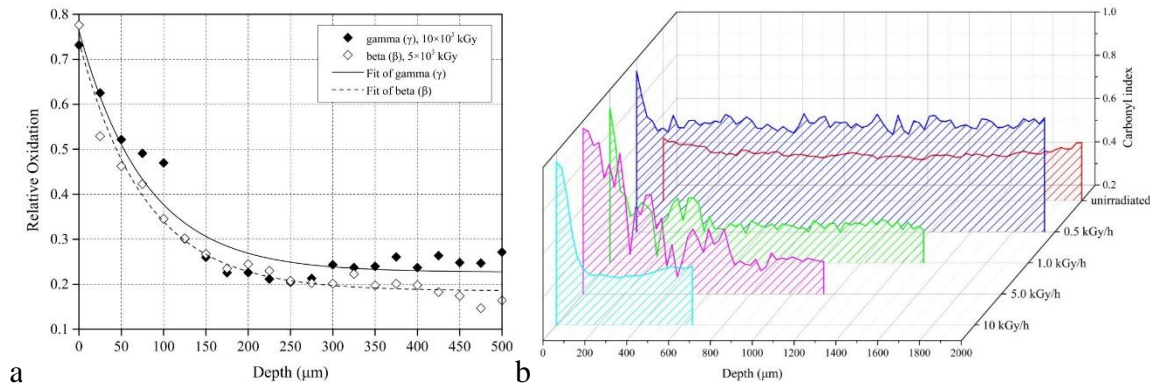


Fig.2 Oxidation penetration depth along the thickness away from the surface: (a) from different irradiation types, (b) from different dose rates

Experimental study on mechanical and fatigue behavior of Dissimilar friction stir welded joint

Guosheng Xu, Guoqin Sun
(Beijing University of Technology)
sguoq@bjut.edu.cn

Abstract: Friction stir welding (FSW) is a solid state joining process and because of its numerous advantages over conventional fusion welding, the FSW technology has been successfully demonstrated for the joining of different type materials including high strength aluminum alloys. The purpose of this research is mainly focused on the welding parameters optimization by the mechanical and fatigue properties of joints as well as the behavior of fatigue crack initiation and growth of 2024/7075 alloy dissimilar FSW joints.

In order to producing the dissimilar FSW butt joints, 3 mm thick rolled plates with dimensions of 300 mm long and 150 mm wide of 2024-T4 and 7075-T6 aluminum alloys were selected, and the specimens for tensile and fatigue test were cut using wire-cut machine. The transverse section of these specimens were ground with carbide abrasive papers of grit sizes from 240 to 3000 for microstructure analysis. The specimens for tensile tests were performed with a displacement rate of 0.6 mm/min, and specimens for fatigue test were performed on electro-hydraulic servo universal testing machine MTS858 under stress controlled sine-wave loading mode at a stress ratio of 0.1 and frequency of 10 Hz. The short cracks were observed with the cellulose acetate film replica technique. The fatigue test was temporarily paused after a certain cycle intervals, and then the tensile load of 80% maximum stress was kept in order to making the fatigue crack in a fully open position when the cellulose acetate membrane was pasted on the joint surface. Finally, the surface crack traces were permanently recorded in the cellulose acetate membranes, and approximately 25-30 dried membranes should be obtained for each surface of joint during the whole fatigue life.

The mechanical properties of joints and the characteristics of short cracks have been investigated. The main conclusions are as follows:

The best quality of joints were obtained with highest tensile strength of 436 MPa when the rotational speed was 900 rpm and the traverse speed was 100 mm/min by placing the 2024 alloy on advancing side and all specimens fractured in A-WZ for tensile test. The statistical results of fatigue specimens showed that more than 70% of specimens fractured in advancing side of weld nugget zone (A-WZ).

The modified crack growth equation using effective crack driving force and semi-elliptical crack projection area parameters is expressed as formula $\Delta K_{\text{eff}}=0.65\Delta\sigma_{\text{eff}}\sqrt{\pi\sqrt{\text{area}}}$. The corresponding result is shown in Fig.1. It indicates that the crack growth rate along with effective stress intensity factor range performs a good correlation. It appears the phenomenon of crack arrest when the effective stress intensity factor is less than 1.3 MPa/m, and the crack growth rate decreases where the coalescence of adjacent cracks with the same effective stress intensity factor.

Based on the results of replica technique, the conclusion shows that the stage of initiation and stable growth of short crack accounts for approximately 55%-75% of the total fatigue life, and the short crack length grow rapidly once it reaches the critical crack size of approximately 350~400 μm . The fluctuation of short crack growth rate can be observed in Fig.2 and it performs retardation before and after the coalescence of adjacent cracks.

This work is financially supported by the National Natural Science Foundation of China (Grant No. 11672010) and the Basic Research Fund Project of the Beijing University of Technology.

Keywords: friction stir welding, dissimilar, mechanical properties, replica, short crack

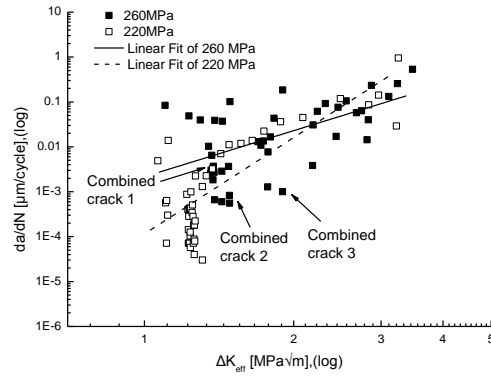


Fig.1 Small fatigue crack growth rate versus effective stress intensity factor

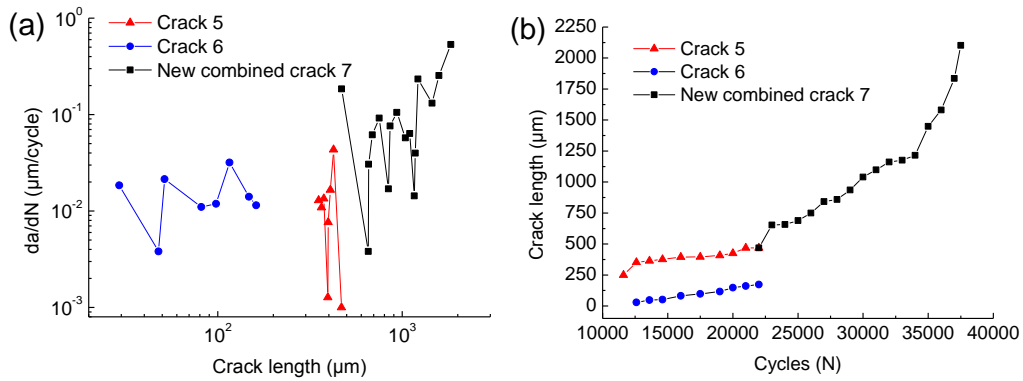


Fig.2 Variations of (a) crack growth rate and (b) crack length along with cycles at the stage of coalescence under stress level of 260 MPa.

Failure analysis on abnormal combustion of transformers in offshore wind turbines

Yimin Zhu, Zhenguo Yang
(Fudan University)
zgyang@fudan.edu.cn

Abstract: With extremely rich offshore wind energy, China has already passed Denmark in 2016 to achieve the third place in the global offshore wind market and 1.6 GW offshore wind power has installed, which accounts for 11% of total installed capacity in the world. However, the offshore transformers are faced with corrosion problems due to the presence of salt and moisture present in the atmosphere. Thus, the safety evaluation of the 1.6 GW offshore wind turbines currently under operation really has an instructive value for those upcoming ones. As an important part in wind turbines, the transformer is used to step up the lower output voltage from the generator to the higher distribution voltage level, and it is regarded as one of the sensitive and weak components in a wind farm. Although much effort had been devoted into the reliability analysis of the offshore wind turbines, as well as the substantial study of failure cases, most of them focused on the failure analysis of structure components, rarely had transformers been reported. Indeed, in the first 3 years after starting commercial operation (from 2014 to 2016) of the 4 MW offshore wind turbines in the eastern part of China, the windings and lead bars installed in the transformer were encountered with failure incidents including ablation and abnormal resistance rise, substantially less than their design lifetime 25 years. Hence, immediate determination of the causes of these premature failures was extremely required to avoid further economic losses and safety problems. Actually, offshore wind turbine transformers are faced with various electrical problems like variable loading cycles, fault current and voltage variations, mechanical problems like vibrations, cooling and insulation failures, and corrosion related problems. However, the reported failures primarily owed to unqualified material and improper operation while only a little emphasis was laid on the fabrication of components and general maintenance, which were also determinants of reliable supply of electrical energy. In this case, based on our previous successful failure analysis experiences on industrial equipment, systematic study on the failed transformers of 4 MW offshore wind turbine was carried out. By various techniques, including temperature simulation experiment, optical microscope (OM), three-dimensional stereomicroscope (3D SM), scanning electron microscope (SEM) and energy disperse spectroscope (EDS), detailed analysis mainly focus on the factors that affect on initiation deterioration of the connection structure of windings and lead bars, on the basis of microscopically analyzing the copper and aluminum composite plates of three phase windings in the same transformer. As a result, corrosion effects leading to different deterioration appearance on the three composite plates were comparatively discussed. The operating temperature of a virgin copper and aluminum composite plate in the transformer was up to 125 °C under normal conditions. Although the deteriorated plates caused abnormal temperature rise, the ablation would not happen unless the installation was inappropriate. Besides, there existed some crevice between the composite plates and copper bars owing to the warping produced during their manufacturing process. It was such kind of the crevice that resulted in occurrence of crevice corrosion and high-temperature oxidation. The interaction between them was the root cause of the failure.

And finally, the prevention methods were proposed. The fabrication of copper bars should be up to standard including flatness and bend angle firstly, and then conductive adhesive should be used to replace the composite plates. It would fill possible crevice and eliminate both corrosion and oxidation. The achievement of current study has a certain reference value for the offshore wind turbines with similar designs and service conditions in China.

Keywords: failure analysis, offshore wind turbine, transformer, combustion

Magnetic plug fracture in gearbox of high speed train

Anxia Pan¹, Zhenguo Yang², Fengzhang Zhang¹, Luoping Xu¹

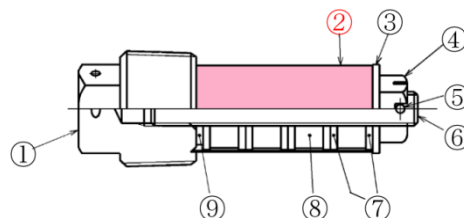
(1. CRRC Qishuyan Institute Co., Ltd.; 2. Department of Material Science, Fudan University)
pax508@126.com

Abstract: Gearboxes are one of the most important components in railway vehicle with regard to safety. The magnetic oil bolt is mounted in the gearbox, which can absorb the metal wear particles formed during gear meshing in order to reduce the wear particles of gears in lubricating oil, and improve the service life of the gear box. The composition of the magnetic oil bolt is shown in Fig.1. Epoxy resin binder between brass sleeve and magnet. The both ends of the brass sleeve are fastened by nuts and gaskets. In this event, the longitudinal cracks were found in several brass sleeves outside the magnetic oil bolt during a regular inspection of 600,000 km for the trains, and the hidden dangers may be appeared during continuous running. The procedures of failure analysis as below:

- 1) The cracks in the brass sleeve were opened and observed by scanning electron microscope, there was corrosion overlay on the fracture, transgranular form on the fracture inner side, and dimple on the outer side, which indicated that the crack originated from the inside and corresponded with the characteristic of stress corrosion crack.
- 2) According to the results of material analysis, the chemical compositions of the brass sleeve meets the national standard requirement of HT62. The metallographic structure of the brass sleeve copper is twin α phase, no coarse grain was observed, therefore the material was qualified.
- 3) According to the residual stress test by patch method, it is found that the axial compressive stress of the brass sleeve was about -80 MPa, and the radial tensile stress is about 79 MPa after the both end nuts of the brass sleeve are fastened by 8 N m torque. The direction of tensile stress is perpendicular to the crack.
- 4) The bonding agent between brass sleeve and magnet is composed of Epoxy Resin Binder and hardener. Tested by Infrared and Raman spectra, the main agent is Bisphenol A Epoxy Resin, the hardener is polyamide, and their heat resistance is poor.
- 5) The heat preservation test of the cured binder was carried out, and the holding temperature was set at 90 °C, which was the temperature of lubricating oil during the service of the gearbox. After 1 h of heat preservation, it was found that a large amount of ammonia was volatilized from the binder.

The analysis results show that the failure mode of brass sleeve is stress corrosion cracking. The temperature resistance of the binder inside the brass sleeve cannot meet the usage requirement, and the amines were volatilized at the service temperature of the gearbox, which should be the root cause of this failure. After the replacement of a new epoxy resin curing agent with higher temperature resistance, no similar cracking occurred.

Keywords: magnetic plug, high speed train, gearbox, stress corrosion cracking



①Screw plug with hex head; ②Brass bush; ③Gasket; ④Hex nuts; ⑤Cotter pin; ⑥Axis; ⑦Magnetic plate; ⑧Magnet; ⑨Gaske

Fig.1 The composition of the magnetic oil bolt

Failure analysis of wear and tear on GCr15SiMn rolling bearing steel

Xiaomei Chen, Huiqiang Wang
(Hebei Agricultural University)
whq@hebau.edu.cn

Abstract: Rolling bearing is one of the important mechanical foundation parts, bearing operating conditions directly affect the quality of the host operation. Rolling bearings are subjected to large alternating loads and extreme contact stresses during operation. They are subject to severe friction and wear. They are subjected to impact loads, corrosion of the atmosphere and the lubricating medium. These factors can cause rolling bearing failure. The so-called failure of the bearing, that is, the bearing loses its prescribed function during work, leading to failure or failure to work properly. Therefore, this requires that the bearing steel must have high and uniform hardness and wear resistance, high contact fatigue strength, sufficient toughness, and corrosion resistance to the atmosphere and the like. Rolling bearing steel is mainly used to manufacture inner and outer rings and rolling elements of rolling bearings. Rolling bearing steel is mainly used to manufacture inner and outer rings and rolling elements of rolling bearings. It can also be used to make certain tools such as measuring tools, molds and so on. GCr15SiMn steel as a high-carbon chromium bearing steel, is used to manufacture inner and outer rings and rolling elements of large rolling bearings, GCr15SiMn steel adopts the heat treatment process of quenching and low temperature tempering. Since the quenching cooling rate cannot meet the requirements, it will not achieve good comprehensive mechanical properties, and will cause the failure of the rolling bearing. Through the analysis of bearing failure, we can intuitively find out the factors of bearing damage, and easy to find out the root cause of bearing failure.

A large rolling bearing in the factory experienced serious wear of the inner ring of the bearing during use, as shown in Fig.1(a). The chemical composition inspection, fracture microscopic examination, non-metallic inclusions test, hardness testing and metallographic examination of GCr15SiMn steel were carried out by direct reading spectrometer, scanning electron microscope (SEM), energy spectrometer, Rockwell hardness tester, optical microscope and stereo microscope. The results show that there are more inclusions of iron containing metal oxides in the wear zone, as shown in Fig.1(b), and the microstructure of the wear zone is granular carbides, hidden-needle tempered martensite and black troostite, as shown in Fig.1(c). The presence of black troostite in the inner ring of the worn bearing is due to the slow cooling process of quenching, precipitation of black troostite along the original austenite and still existing organization after low temperature tempering, whereas the presence of black troostite will reduce the hardness of inner ring of worn bearing, the low hardness of the inner ring of the worn bearing can lead to plastic deformation at the wear zone, as well as indentation, cracks and holes are caused by plastic deformation, the concentrating effect of these factors led to the failure of GCr15SiMn steel large rolling bearing.

Keywords: GCr15SiMn, troostite, non-metallic inclusions, plastic deformation

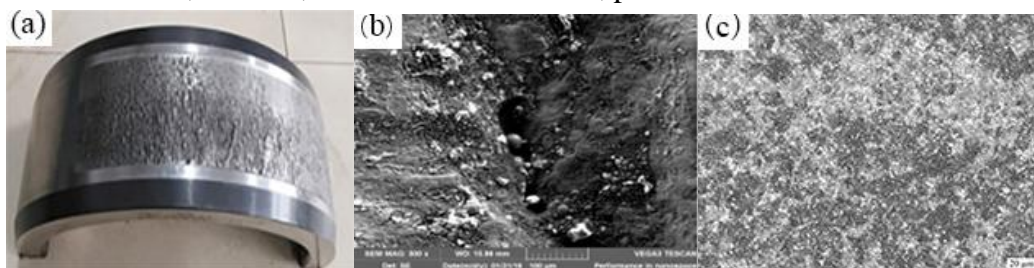


Fig.1 worn bearing inner ring: (a) macro-morphologies of the worn bearing inner ring; (b) micro topography of the worn bearing inner ring; (c) microstructure of the worn bearing inner ring

Finite element simulation on the vibration failure of rigid polyurethane foam at high temperature

Jiacheng Wu, Zhiqiang Yu
(Fudan University)
yuzhiqiang@fudan.edu.cn

Abstract: The vibration failure mechanism of rigid Polyurethane foam (RPUF) at high temperature was investigated by finite element simulation. The finite element model was established by ABAQUS to study stress distribution of RPUF under vibration load. Hyperelasticity material model was used to describe mechanical behavior of RPUF by Mooney-Rivlin model through uniaxial test data at 150 °C. An alternating tensile load with amplitude was applied on one side of tensile spline for vibration simulation, while another side was totally fixed. The amplitude of tensile load was calculated by the equation as followed: $F_{(t)}=F_0[\sin(\omega t)+1]$, where $F_{(t)}$ indicated force (N) that depended on time (s); ω was angular frequency and F_0 represented initial force at 100 N.

The assembly was discretized by 12,238 hexahedral elements (C3D8R, three-dimensional, 8 nodes, reduced integration) and 8,199 wedge elements (C3D4, three-dimensional, 4 nodes). Fig.1 illustrated the vibration stress distribution of the tensile spline under vibration of 1000 Hz, and it was obvious that a stress concentration existed in the cells about 15000 Pa, significantly exceeding the part with no cells. As shown in Fig.2, the partial enlarged contour was utilized to show stress annular distribution in cells. The micro cells in RPUF could be regarded as some micro defects, and stress concentration easily occurred under tensile load. The stress concentration on cells resulted in formation and propagation of micro cracks around cells during vibration process. Therefore, some cells were destroyed when the micro cracks got coalesced, and then open-cell structure was easily formed. For model verification, the tensile test was utilized to evaluate vibration damage degree at 150 °C of RPUF by tensile strength and modulus. Aged RPUF specimens were prepared with different vibrational frequency ranging from 0 Hz to 2000 Hz at 150 °C for 30 min. At low vibrational frequency, the tensile strength and modulus was almost unchanged, while they decreased significantly at high vibrational frequency. The SEM analysis of the tensile fracture surfaces revealed that the vibration failure of RPUF at high temperature was mainly resulted from the destruction of cell structure. At high vibrational frequency, most of cells were destroyed, and open-cell structure was observed, which explained the stress concentration in finite element simulation through microstructure. Combined with the decrease of tensile properties and SEM analysis, the finite element simulation proved the existence of cell structure increased the possibility of vibration damage due to concentration of vibration stress on cells.

Keywords: failure mechanism, finite element simulation, cell structure, vibrational frequency, high temperature

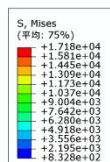


Fig.1

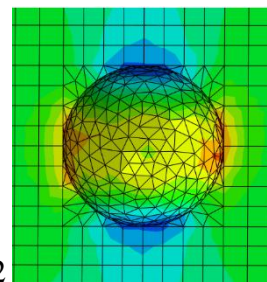
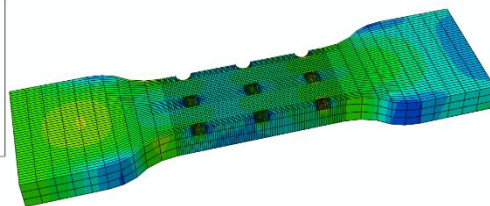


Fig.2

Fig.1 Vibration stress distribution of RPUF under 1000 Hz at 100 N

Fig.2 Partial enlarged contour of vibration stress distribution in cells

Numerical study of mechanical properties of straight pipe and elbow during in-service welding

Ling Qiao, Tao Han
(China University of Petroleum)
hantao_upc@163.com

Abstract: Pipelines have been widely employed as one of the most economical and practical ways for oil and gas transportation over long distance. Pipelines are usually subjected to complex combination of straight pipe and elbow. And elbow has become an important part in pipeline network due to its excellence of changing the flow direction of medium. However, elbows are the most vulnerable parts in pipeline network systems. The residual stress for in-service welding repair has significant impacts on the mechanical properties of straight pipes and elbows. In this paper, X70 pipeline is employed and the thermal elastic-plastic finite element method is performed to investigate the mechanical properties of the straight pipes and elbows during the in-service welding. To ensure the accuracy of the simulation, a double ellipsoid heat source is employed and the heat source is fitted repeatedly to guarantee that the results of the temperature field could agree well with the actual molten pool. The predictions of residual stress and deformation distribution in the straight pipes and elbows are performed based on the validation of the numerical models. And the effects of the curvature radius and defects on the elbow are investigated. Three sizes of the curvature radius is provided to investigate the residual stress and deformation distribution in the elbows. And by orthogonal experiment, various sizes of defects are presented in the elbow to study the effect of defect size on the mechanical properties of the elbow.

The results show that an accurate temperature field of in-service welding is provided to investigate the mechanical properties of fillet joint. The residual stress distribution is uneven along various directions after welding. It is tensile near the weld region and increases with the decrease of the distance to the weld. The deformation and residual stress at the mid position is less than two ends of weld center line along the direction of the welding line. It could be deduced that the middle position of the circumferential weld is most vulnerable to failure. And the residual stress descends from top to bottom along the thickness direction due to the difference in temperature and heat exchange. Furthermore, the deformation and residual stress increases with the decrease of the curvature radius. And compared to the intact elbow, the residual stress in the elbow with defects increases significantly in the defective area. The von mises residual stress shows tensile and the hoop residual stress shows compressive. And the results obtained by orthogonal experiment show that the depth and length along the axis are the main factors affecting the mechanical properties of the elbow. An important implication can be obtained that the residual stress becomes important if deep corrosion is detected in practice. This paper makes a systematic analysis of the mechanical properties of straight pipes and elbows in the process of in-service welding repair. And it can provide useful guidance for the elbow repair.

Keywords: in-service welding, elbow, residual stress, curvature radius, pressure, defects

Service experiences with cracking in T23 weldments

Jeff Henry

(ATC-Engineering Services)

jhenry@atc-tn.com

Abstract: For over 50 years, the conventional Cr-Mo steels, such as Grades 11 and 22 have been used in large utility-type boilers throughout the world with notable success. From this solid base of experience there has emerged a new group of high-strength ferritic materials that offer substantial improvements in elevated temperature performance through the judicious addition of a range of precipitate-forming elements, such as columbium, vanadium, titanium, tungsten, nitrogen, and boron. Following in the footsteps of the German X20 material, Grade 91 rivals TP304H in high-temperature strength up to approximately 1150 °F. A more recent addition is the low carbon modifications of Grade 22, designated Grades 23 and 24, which were developed to be highly weldable grades that could be left in the as-welded condition, in contrast to Grade 91. Laboratory tests have confirmed the improved weldability of Grade 23, with relatively low hardness values possible in as-welded condition. However, service experience with this alloy has been very limited, except for tightly controlled trial applications conducted by the OEM/steel mill partners. As a consequence, its behavior outside of the laboratory, under the less felicitous conditions that typically prevail in a modern power plant, naturally is of some interest.

With increasing applications of T23, cracking issues in Grade 23 welds have become a “hot topic” over the entire utility industry. During the recent commissioning of a new supercritical utility boiler with a portion of the furnace constructed using T23 tubing, a number of problems were encountered in the furnace that largely were confined to the T23 tubing. Subsequent analysis of samples of failed tubing proved conclusively that the problems encountered did not reflect an inherent weakness of the T23 material, but that problems would have occurred to some degree had one of the standard alloy steels been installed at the failure locations under similar conditions of processing. The analysis did suggest, however, that claims made by the tube supplier regarding the virtual immunity of the as-welded material to damage such as welding “cold” cracks or stress-corrosion cracking were exaggerated. In particular, it was found that under exceptional conditions T23 material in the fully hardened condition could attain hardness levels sufficiently high to render the material susceptible either to hydrogen-assisted cold cracking or to stress corrosion cracking. In the following discussion, the history of some T23 weld cracking incidents is recounted, and the results of the analysis of the damaged tubing are reviewed in detail.

Keywords: T23, cracking, welds

Thermally grown oxide (TGO) formation and growth in doublelayered composite thermal barrier coating and failure mechanism analysis

Ran Wang¹, Yuelan Di¹, HaiDou Wang¹, Tianshun Dong², Guolu Li², Li Liu²
(1. Academy of Armored Forces Engineering; 2. Hebei University of Technology)
15811583556@163.com

Abstract: Nickel-based heat resistant alloy are usually used for application with high temperature, it can withstand a maximum temperature of 1200 °C. this is usually below the temperature requirement for severe working conditions. Furthermore, it is difficult to improve its overall high temperature oxidation resistance. Thermal barrier coatings are widely used in aerospace engines due to their low thermal conductivity, excellent thermal insulation properties and high resistance to increasing temperature oxidation. Thereby, thermal barriers helps reducing energy consumption and resource waste.

In this paper, thermal barrier coatings (TBCs) were prepared by atmospheric plasma spraying technology. The ceramic coatings were a single layer of 8YSZ (Y₂O₃ partially stabilized ZrO₂) and a double layer of 8YSZ and lanthanum zirconate (LZ). Another double-layer coating was used to inspect the thermal insulation performance and high-temperature oxidation performance. The thermal insulation properties of the barrier coating and the microstructure growth behavior of the thermally grown oxide (TGO) were investigated at high oxidation temperature. Experiments showed that the thermal insulation performance of YSZ+LZ double-layered ceramic coating is significantly higher than that of YSZ singlelayered ceramic coating. The oxidation growth of TGO was the main failure reason of thermal barrier coating. The growth rate of TGO in the thermal barrier coating was faster in the initial stage of high temperature oxidation, however the growth rate of TGO began to decrease with the increase of oxidation time. The thermal barrier coating system (TBCs) of YSZ+LZ structure had high bonding strength with the bonding layer, and the preparation of pyrochlore thermal barrier coating on YSZ improved the TBCs overall stability at higher temperature and reduced the oxidation tendency. Finally, in order to overcome the coating instability caused by the reaction of pyrochlore with Al₂O₃ in the TGO under high temperature conditions, YSZ+LZ TBCs was introduced and proved to have better performance stabilizing the system at those temperature sets.

Keywords: double thermal barrier coating, TGO, high temperature resistance, failure mechanism

Failure analysis of excessive corrosion in wastewater treatment reactor

Bo Zhao¹, Changfu Fan², Jing Guo¹, Yuxin Yu¹, Tianyu Zhou¹, Tong Xu¹

(1. China Special Equipment Inspection and Research Institute; 2. Bluestar Machinery Co., Ltd.)
zhaobo19840626@163.com

Abstract: In this article, macromorphology, micromorphology, chemical composition, metallography, fracture morphology, and parallel test were used to analyze the excessive corrosion of tube and coupons were made of Inconel 625 alloy in wastewater treatment reactor. Macromorphology showed that serious pitting distribute both on the outer surface of coupons and inner surface of tube, and showed a shallow dish shape with great length diameter ratio. The pitting distributed densely and linked together to ulcerative corrosion morphology, which is the main reason for materials thickness decreasing. It can find a large amount of chromium-rich carbide at grain boundaries in micromorphology and metallography testing, and showed severe sensitization of grain boundary. Because of that the corrosion behavior mainly attribute to the intergranular corrosion. The parallel test showed that it could reduce the resistance to intergranular corrosion rapidly by increasing of the carbon content, and the quality of solid solution treatment also had significant impact on it, although their chemical composition all correspond to the standards' requirements.

According to the results and references, Inconel 625 alloy was achieved the limits of anticorrosion properties in this environment, and excessive wide of chemical composition requirements might cause excessive corrosion in harsh environments, especially for nickel base alloy and heat treatment in automatic assembly line. If the process parameters are not varied, this reactor need replace materials with low carbon of Inconel 625 alloy or higher grade of corrosion-resistant alloys, and need applicability evaluation with environmental simulation experiments.

Keywords: failure analysis, Inconel 625 alloy, intergranular corrosion

Failure analysis of angular contact ball bearing in a boosting pump of nuclear power plant

Qun Ding, Zhenguo Yang
(Fudan University)
zgyang@fudan.edu.cn

Abstract: A premature failure of angular contact ball bearings in boosting pump for condensate water of a nuclear power plant was investigated. After disassembly, cages of the two bearings were found to be failed: one was broken into pieces and the other suffered severe distortion. Operation conditions, installation design, materials quality and macro/microscopic observations of the failed bearings were carefully studied. It turned out that the surface of the steel balls and inner races underwent serious abrasion. There were black traces on the edge of the bearings indicating that the failed bearings once encountered overheating and poor lubrication which was also evidenced by experimental simulation. It was concluded that the three-body abrasion induced by small axial clearance among the steel balls, inner race and outer race was the root cause of premature failure of bearings. The relevant failure mechanisms of the two bearings were carefully discussed and effective countermeasures were put forward as well.

Keywords: angular contact ball bearing, nuclear power plant, failure analysis, three-body abrasion, axial clearance

Failure analysis of leakage of valve tube in drain pipeline in nuclear power plant

Rong Wang, Yangyang Fu

(Testing Center of Shanghai Research Institute of Materials)

wangrong1967@126.com

Abstract: The leakage of the valve tube in drain pipeline in nuclear power plant was found during use. Its material was 15CrMo. Normally, the upper end of the valve was purified water, the temperature was 260 °C, the pressure was 4 MPa, and the lower end of the valve was negative pressure (approximately 1 atmosphere). The leak location is located at the lower end close to the valve body. The failure analysis and physicochemical analysis results of the valve tube leakage show that the water flowing into the cavity of the valve core passes through the wear groove on the spherical sealing of the valve tube, forming a high velocity water jet and then forming turbulent flow on the wall surface of the valve tube, resulting in FAC, which causes the valve tube wall to penetrate and leak.

Keywords: valve tube, flow accelerated corrosion, leakage, nuclear power plant

Failure analysis of leaking small-diameter buried 20 steel pipe

Caihong Lu

(Tubular Goods Research Institution)

lucaihong@cnpc.com.cn

Abstract: In this paper, non-destructive testing, component analysis, mechanical properties testing, microstructure analysis, electrochemical detection and soil corrosion analysis were used to failure analysis of the leaking small-diameter buried 20 steel pipe. The results show that the main reason for the leakage of the steel pipe is the mechanical damage. The outer layer of the pipe was peeled off, resulting in leakage of oxygen corrosion in the pipe body.

Keywords: small-diameter buried pipe, failure analysis, mechanical damage, oxygen corrosion

Helicalspring fracture failure analysis of suspension for vehicle

Aofan Liu, Wenchang Huang, Yong Li, Yue Zhang

(Dongfeng Motor Corporation Technical Centre)

liuaf@dfmc.com.cn

Abstract: Helicalspring in suspension for vehicle fractured after an endurance test in a relatively severe environment. The fracture mode and causes were investigated by means of chemical composition analysis, microstructure, microscopic observation and hardness test used by optical microscope, optical emission spectrometer and other instruments, also the working condition, manufacture process and finite element method analysis were considered. The result show that rupture of helicalspring is low cycle fatigue fracture which happened due to surface decarburization by abnormal heat treatment and poor blanking quality of side surface. Furthermore, some effective improvements were put forward and achieved nice consequence.

Keywords: helicalspring, 60Si2Mn, surface quality, fatigue fracture, heat treatment

Peridynamic simulation of crack formation and propagation in pitting corrosion of carbon steel pipes

Qi Tong¹, Chunxiang Shi², Yi Gong¹, Zhenguo Yang¹
(1. Fudan University; 2. Shanghai Institute of Technology)
tongqi@fudan.edu.cn

Abstract: Stress corrosion cracking (SCC) is the initiation and propagation of crack due to the combined effect of stress and corrosive environment, which may substantially lower the strength of the materials and lead to unexpected failure. Specially, pitting corrosion is an extremely localized corrosion style, where micro cracks are easily formed. While characterization tools such as scanning electron microscope (SEM) and energy disperse spectroscope (EDS) are harnessed to identify the specific issues, numerical simulation is capable of handling complicated working conditions and monitor the dynamic process. Moreover, computational prediction is suitable in guiding the design process and to avoid the disasters in advance. In recent years, a nonlocal continuum model called peridynamics has been developing and demonstrating its advantages in modeling dynamic fracture. Different from mesh-based methods, peridynamics calculates forces on material particles in an integral form, which is still valid in the presence of discontinuity. Therefore, crack initiation and propagation are inherently captured without a priori knowledge. To this end, we present numerical study of SCC in corrosion pits based on peridynamic modeling in this paper. The simulations are implemented based on carbon steel pipes in different engineering environments and conditions such as in heat exchanger of ethylene plant. We focus on the dynamic propagation of cracks nucleated from corrosion pits with different sizes and layers due to various conditions, and analyze the failure patterns. The results are compared with the records of field inspection cases, which show the promise of numerical predictions in the fields of failure analysis and engineering design.

Keywords: stress corrosion cracking, peridynamics, pitting corrosion

Failure case analysis—failure analysis of casing head slip hanger

Zhi Zhang¹, Pengfei Sang¹, Zhipeng Sang², Zhe Zhang¹, Jing Li¹, Yushan Zheng¹
(1. Southwest Petroleum University; 2. CCDC Tarim Engineering Company)
798272782@qq.com

Abstract: The workpiece failure fracture happens frequently in oilfield because of the poor environment and the complex working conditions. The main function of the slip hanger is to hang the casing in the wellbore. It is an important part of the casing head. This paper brings a failure case study of casing slip hangers. The main reasons for failure fracture of casing slip hangers have been proposed based on the analysis techniques of continuum analysis, chemical composition test, metallographic analysis and mechanics performance testing. The results show that the charpy impact toughness of slip hangers material is lower at low temperature is lower. The impact curve is the characteristic curve of brittle fracture. reflects the fracture has no plastic zone. There are more ferritic bodies due to the material organization is not completely transformed into a well-performing sorbite. The material fracture surface was seriously polluted by environmental media. The fracture features were developed by the transgranular ductile fracture to the intergranular brittle rupture. The summary of this study indicates that the slip hanger fracture failure because of the crack in root of thread, which result from compound effect of additional load, the stress concentration of the thread and the pollution of environmental media accelerates crack propagation.

Keywords: failure analysis, slip hanger, trans-granular fracture, intergranular fracture

Failure analysis of welded chain slings used for lifting purpose in oil and gas industry

Juntao Yuan

(Tubular Goods Research Institute of CNPC)

yuanjuntaolly@163.com

Abstract: Various means were used to analyze the fracture causes of the welded chain slings used for lifting purpose in a western oil field. Physicochemical analysis indicated that the chemical composition of the chain was similar to that of 20Mn2 alloy steel, the microstructure was mainly martensite with localized bainite in the vicinity of the fracture, the grain size was 8.5, no excess inclusions were present, and the hardness near the fracture was slightly lower than that of the suspension chain. Micro-analysis showed that there were a large number of inclusions in the area near the outer surface of the fracture source, containing high Mn and Si content. Combined the experimental analysis with the manufacturing process of the chain, the fracture causes of the welded chain can be clarified as follows: quenching was applied to the chain to obtain the martensitic structure with high strength and hardness, however, a large number of Mn and Si inclusions as well as local upper bainite structures formed in the welding process would greatly reduce the bearing capacity; when the chain suffered greater load or sudden impact during the service process, the fracture occurred at the weld first.

Keywords: chain, fracture, bainite, inclusions, weld

Investigation on impact absorbed energy index of drill pipe

Fangpo Li

(CNPC Tubular Goods Research Institute)

lifangpo@cnpc.com.cn

Abstract: Drill pipe is one of the most important tool for petroleum and natural gas drilling exploitation. The application of S135 drill pipe can significantly increase drilling depth, reduce drilling cost and improve drilling quality. Impact absorbed energy is the most important toughness index, which has decisive influence on drill pipe's failure mode. Statistical result of ninety-one drill pipe failure cases shows that piercing is the mainly failure mode of S135 drill pipe, which includes oval-shaped piercing and slot piercing. Oval-shaped piercing hole's length is mainly distributed in 20-50 mm, and their impact absorbed energy disperses in 42-156 J. Slot piercing hole's length is mainly distributed in 60-90 mm, and their impact absorbed energy concentrates in 76-150 J. Analysis result shows that there is certain correlation between the piercing hole's length and drill pipes' impact absorbed energy value. In the paper, the impact absorbed energy index calculation formula for drill pipe's "leak before break" failure mode is proposed. The results show that the impact absorbed energy value increases with the increasing of critical crack length, stress strength coefficient square, and strength grade. The impact absorbed energy value of S135 steel drill pipe should greater than 80 J in order to ensure drill pipe's service safety.

Keywords: drill pipe, S135 drill pipe, failure mode, piecing failure, impact absorbed energy

Failure analysis of sulfide stress corrosion cracking on P105 tubing coupling

Yan Han

(CNPC Tubular Goods Research Institute)

hanyan003@cnpc.com.cn

Abstract: String falling was caused by the tubing coupling cracking in the Western Oilfield. In this paper, the macro-analysis, the physical, chemical properties, metallographic, scanning electron microscope (SEM), energy dispersive spectrometer (EDS), X-ray diffraction (XRD) and sulfide stress cracking resistant (SSC) test were used to analyze the failure mechanism of the coupling. The results showed that the cracking of the coupling is mainly sulfide stress corrosion cracking which is caused by the hydrogen sulfide in the well. This type material is not suitable for use in the sulfur environment.

Keywords: tubing coupling, sulfide stress corrosion cracking, failure analysis

Experimental study on temperature effect of high performance casing material in deep well and ultra-deep well

Wenhong Liu¹, Dashun Qin², Zhiyong Pan³, Kai Lin³

(1. State Key Laboratory for Performance and Structure Safety of Petroleum Tubular Goods and Equipment Materials, CNPC Tubular Goods Research Institute;

2. Northwestern Polytechnical University; 3. CNPC Tubular Goods Research Institute)

dashun_qin@163.com

Abstract: With the exploitation of deep well, ultra-deep well, thermal recovery Well and Geothermal Well, the casing's service temperature is increasing constantly. The influence degree of temperature on casing material performance has attracted much attention in the design of casing strings. The experimental study on the yield strength and tensile strength of casing materials with temperature change is carried out, which includes C110, 140 ksi and super13Cr 110 ksi casing. In this paper, the yield strength correction coefficient of casing material is defined, and the material performance model of different steel grade casing material with temperature change is established. The paper describes the influence of underground high temperature on the design of casing strings and shows that the yield strength of casing material will decrease under high temperature. This directly affects the safety parameter of casing design, and greatly impact on the safety reliability and service life of the casing strings. This paper points out the defects which exists in the current API formulas, when calculating the force of the casing string. It is suggested that the yield strength at high temperature should be used as the design basis for deep well and ultra-deep well when the underground temperature is high. The results can be used to guide the design and check of casing strings and tubing strings under high temperature and high-pressure gas well.

Keywords: deep well and ultra-deep well, high performance casing, high temperature, yield strength, well strings integrity

Fracture control of the 2nd west east gas pipeline

Yaorong Feng

(Tubular Goods Research Institute of CNPC)

fengyr@cnpc.com.cn

Abstract: The 2nd west east gas pipeline (2nd WEGP) is the first major pipeline project in China importing abroad natural gas resource and also the longest and largest quantities gas transmission line in the world with gas supply of middle Asian natural gas and adjusting gas supply of domestic gas from Tarim Basin and Ordos Basin. The primary target market is south china not covered by previous the 1st WEGP, and the market of North and East China is also taken into account through branch of the 2nd WEGP. It has one artery and 8 branches, starts at Khorgos of Xinjiang province, goes by way of provinces/districts/cities and finally reaches Hongkong. Its total length is 9000 km, in which the total length of artery from Khorgos to Guangzhou is 4900 km. Its design throughput is 30 billion cubic meters per year and its total investment is 142 billion RMB. The 2nd WEGP started at February 2008 and completed at December 2012.

Designed maximum operation pressure of the 2nd WEGP is 12 MPa, largest diameter of pipe is 1219 mm and highest steel grade is X80. To ensure the long-term security and reliability in operation, fracture control program has been proposed through systematic research, including crack initiation control, brittle fracture control and ductile fracture control. The requirement of arrest toughness of the 2nd WEGP had been studied on the basis of pipe full-scale burst test data base in the world, Battelle two curve method (BTCM) and GASDECOM software. Full scale burst tests of X80 high-pressure gas pipeline had been successfully performed based on previous research results. The fracture control program of the 2nd WEGP was set up based on different fracture criteria and the principle of both security and economy. The arrest ability of X80 spiral submerged arc welded (SSAW) pipe was firstly verified and a new correct factor of arrest toughness prediction was obtained. Results presented that the arrest ability of SSAW pipe is better than longitudinal submerged arc welded pipe. It is also indicted that the absorbed energy of drop weight tear test (DWTT) can accurately reflect full-scale fracture behavior of pipe, a inverse relation between fracture separation and arrest ability of pipe and an absorbed energy of DWTT required by fracture arrest is presented.

Keywords: the 2nd west east gas pipeline, fracture control

Fracture failure analysis on ultra supercritical turbine bolts

Nan Li

(Central Iron and Steel Research Institute)

linan@necast.com

Abstract: Fracture failure analysis on ultra supercritical turbine bolts was carried out by means of chemical composition analysis, mechanical properties testing, metallographic examination and fracture analysis. The results show that the main reason of the bolts fracture is high temperature stress-rupture, with the fracture morphology being intergranular cracking character. The main fracture is perpendicular to the axial direction of bolt, which indicates that the tensile working stress result in the crack. In addition, another kind of cracks which is 45 °of the axis has been found on the bolt. It indicates that there must be some abnormal torsion stress on the bolt which most possibly be caused during assembling process.

Keywords: fracture failure analysis on ultra supercritical turbine bolts, intergranular fracture, stress-rupture

Research on the performance of hollow bolt yield ratio of 45 steel

Weilian Sun
(Hebei Agricultural University)
sunweilian@hebau.edu.cn

Abstract: The hollow bolt is an important part of slope reinforcement of buildings such as tunnels, railways, highways, bridge foundations, high-rise buildings and dykes. The annual volume of the steel used for reinforcing anchor bolts is several million tons, and its mechanical properties (Especially the yield ratio) is important for ensuring the safety and reliability of the reinforcement project. Hollow bolts are usually made of Q345B steel with a yield ratio of 1:1.25 and an elongation of up to 21%. In order to save resources and reduce production costs, the 45-steel cold-rolled tube and conventional heat treatment technology were used. The yield ratio of the hollow bolt was low, and the elongation was poor. In order to solve the problem of insufficient performance, Using optical emission spectrometer, metallographic microscope, tensile testing machine and special heat treatment equipment, the composition, microstructure, mechanical properties, plastic deformation and production process were analyzed, and the influencing factors and influence laws of the comprehensive mechanical properties of 45 steel hollow bolts were studied. Through the composition study, the carbon content of 45 steel was adjusted moderately, the appropriate amount of plastic deformation and heat treatment method were select, and the results meet the technical requirements of hollow bolts. Through process improvement, the key technology of high-frequency hot rolling deformation heat treatment is adopted to make the yield ratio and elongation of the hollow bolt body made of 45 steel meet the technical requirements, and it can effectively reduce the production cost and achieve energy conservation and environmental protection

Keywords: hollow bolt, yield ratio, elongation, hot rolling, hollow bolt, yield ratio, elongation, hot rolling

Failure analysis of a P110 grade non-API anti-sulfide corrosion tubing coupling used in ultra deep oil well

Chun Feng
(Tubular Goods Research Institute of CNPC)
steels@qq.com

Abstract: The main reasons for cracking failure of a P110 grade Non-API anti-sulfide corrosion tubing coupling used in a ultra deep oil well have been investigated by chemical composition analysis, mechanical properties test, optical microscopy (OM), scanning electron microscope (SEM), energy dispersive spectrometer (EDS), X-ray diffraction (XRD) and full-scale test. The results show that the composition, structure and mechanical properties and corrosion test of the tubing coupling were all in accordance with the corresponding parameter requirements. Furthermore, it was suggested that stress corrosion cracking (SCC) cracks initiated in the outer wall of joint was caused by the combined effect of sulfide stress corrosion, CO₂ corrosion, acid corrosion and erosion corrosion. The cracks growth and propagation led to the cracking failure. Moreover, the results of microstructure observation indicated that decarburization, band-segregation, and non-metallic inclusions distributed around the fracture surface were the essence of the cracking failure. In addition, a simulation model of the cracking failure was given and strict Non-destructive detection before well completion were proposed for prevention.

Keywords: oil country tubular goods, tubing and coupling, sulfide stress corrosion, failure analysis

A phase transformation to predict the high contact stress in bearing steel due to rolling contact fatigue

Xian Guo, Xu Zhou, Dejie Huang
(Zhejiang Wanxiang Precision Industry Co., Ltd.)
guoxian@jg.wxqc.cn

Abstract: The microstructural changes, such as dark etching region (DER), in the sub-surface of AISI 52100 and SAE 1055 steels are generally attributed to rolling contact fatigue. DER tends to appear after numerous cycles ($>100 \times 10^6$) under relative high contact stresses in the region where maximum shear stress appears, merely knowing that is due to contact fatigue, but the failure mechanism and causes remain to be revealed. This paper focused on the evaluation on the DER in the through-hardened martensitic AISI 52100 inner rings and the SAE 1055 local-hardened martensitic flanges based on their microstructural changes. The microstructure was characterized by optical microscope (OM), SEM, microhardness and X-ray diffraction. The results showed that despite of these two different steels, the residual austenite was decreased indicating its significance in the microstructural changes and the load subjected.

Keywords: rolling contact fatigue, dark etching region, retained austenite, residual stress

Cracking failure analysis on L245NS steel grade elbow

Yuanyuan Zhu, Dongming Yang, Wenguang Zeng, Wenwen Xiao, Yujie Guo
(SINOPEC Northwest Oilfield Company)
zhu_yuan20@126.com

Abstract: The hot bending elbow has many advantages, such as small residual stress, uniform roundness and large adjustment range of bending angle. It is widely used in pipeline engineering construction, which is used to change pipeline laying direction and relieve pipeline thermal stress. Cracking and failure occurred on hot bending elbow only four years after a natural gas pipeline was built and put into operation. Material properties of the bending elbow were tested by means of chemical composition analysis, mechanical property testing and metallographic examination. Fracture surface morphologies and corrosion production were analyzed by SEM and EDS respectively. The results showed that the chemical composition, tensile properties, impact properties and hardness were not consistent with the standard requirements. It also revealed that the macrostructures of inside arc were ferrite and martensite, and the macrostructure of outer arc was martensite, which resulted in higher hardness of the steel. Hydrogen that produced by internal H_2S medium, transfer from the pipe inner surface to outer wall. In this process, stress concentration was produced in surface defect area that influenced by partial extension stress. When the crack extension to a certain degree of residual wall thickness that cannot take pipe pressure lead to elbow cracked. The main reason for the cracking of the bending elbow was hydrogen sulfide stress corrosion cracking.

Keywords: L245NS steel grade, heat-bending bend, cracking, failure analysis

Fracture failure analysis of C110 casing in sour oil and gas field

Yuanyuan Zhu, Xiaoxuan Xu, Wenwen Xiao, Xiuyong Fu, Jie Zhang, Fang Li
(SINOPEC Northwest Oilfield Company)
zhu_yuan20@126.com

Abstract: In order to avoid casing corrosion failure petroleum production by the medium environment such as H₂S, CO₂, Cl⁻. C110 steel was widely used in acid oil and gas field exploration and development. Fracture failure occurred only four years after the casing of an acid oil and gas well was put into operation. Therefore, the C110 steel casing failure analysis was particularly important for acidic oil and gas fields' efficient development. Material properties of the casing were tested by means of chemical composition analysis, mechanical property testing and metallographic examination. Fracture surface morphologies and corrosion production were analyzed by SEM and EDS respectively. The results showed that the material properties were consistent with API SPEC 5CT standard requirements, the failure of casing failure was eliminated by material factors. Casing non-centered was produced a stress concentration, and seriously mechanical damage was formed by casing and slip first biting tooth. At the same time, alternating load was appeared in stress concentration position that caused by stratum movement, casing pressure fluctuation and other factors. The fracture originated from the inner surface of the casing and presented brittle fracture characteristics. The main reason for the fracture of the casing was the corrosion fatigue cracking under the high H₂S, low pH corrosion medium and alternating load.

Keywords: sour oil and gas field, casing, corrosion fatigue crack, failure analysis

EIS studies of the resistance-reducing internal coating of in-service natural gas pipeline

Weifeng Ma
(CNPC Tubular Goods Research Institute)
mawf@cnpc.com.cn

Abstract: Because the internal coating of pipeline unable to examine and check up directly. So, it is particularly important to carry out the dependability assessment and life evaluation for the internal coating of in-service pipeline. The electrochemical behavior of the internal coating of the service five years pipeline in 3.5%NaCl solution was studied by Electrochemical Impedance Spectroscopy (EIS). The result indicated that there is an amount of channels in epoxy coating with five years' service time, which made water molecules could easily reach interface of the coating and matrix metal, leading to the coating resistance decreased quickly. Only after 24 hours, the coating resistance from 109 Ω·cm² quickly reduced to less than 106 Ω·cm². When the coating resistance was decreased to 104 Ω·cm², the coating performance was degraded and the bubbling appeared. The coating impedance model, capacitance and resistance value of coating at different immersion stages were obtained.

Keywords: electrochemical impedance spectroscopy, internal coating, impedance model, equivalent circuit